Space Weather

REVIEW ARTICLE
10.1029/2019SW002195

Special Section:
Scientific Challenges of Space Weather Forecasting Including Extremes

The Great Storm of May 1921: An Exemplar of a Dangerous Space Weather Event

Mike Hapgood[1]

[1]RAL Space, STFC Rutherford Appleton Laboratory, Harwell Campus, Didcot, UK

Key Points:

- A review of scientific papers, newspapers, and other reports is used to build a timeline of the great geomagnetic storm of May 1921
- The first part of the storm created conditions that enabled later activity to cause some of the most severe geoelectric fields on record
- This timeline adds to the knowledge we can use to develop the scenarios needed to plan mitigation of future severe space weather

Supporting Information:

- Supporting Information S1

Correspondence to:
M. Hapgood,
mike.hapgood@stfc.ac.uk

Citation:
Hapgood, M. (2019). The great storm of May 1921: An exemplar of a dangerous space weather event. *Space Weather*, *17*, 950–975. https://doi.org/10.1029/2019SW002195

Received 8 MAR 2019
Accepted 7 JUN 2019
Accepted article online 23 JUN 2019
Published online 22 JUL 2019

Abstract We reconstruct the timeline of the extreme space weather event of May 1921, reviewing a wealth of reports from scientific literature, databases, newspaper reports, and reports by historians and astronomers. A series of coronal mass ejections (CMEs) bombarded Earth between 13 and 16 May, as shown by a series of sudden commencements observed across the global network of magnetometers. These CMEs produced three major periods of geomagnetic activity. The first period followed the arrival of two CMEs on 13 May. These may have cleared much density from the inner heliosphere, enabling a subsequent CME to travel quickly to Earth and cause intense activity. Continuing moderate magnetic activity following the first period may also have preconditioned the magnetosphere so it responded strongly to that later CME. This arrived late on 14 May, driving a short period of very intense activity early on 15 May, including technological impacts indicative of strong geoelectric fields. Another CME arrived early on 16 May, driving intense activity similar to that on 13 May. We show how these impacts fit with scientific observations to give a timeline that can be used in worst-case studies/benchmarks. We also show that some impacts were probably coincidental with the storm, but due to more prosaic faults. This sequence of preconditioning, intense geoelectric fields, and their impacts, plus coincidental faults, makes the 1921 event an excellent basis for building space weather scenarios. Such scenarios are vital scientific input to the development and implementation of policies for mitigation of severe space weather.

Plain Language Summary The severe space weather event of 13-16 May 1921 produced some spectacular technological impacts, in some cases causing destructive fires. It was characterized by extreme solar and geomagnetic variations, and spectacular aurora, recorded at many locations around the world. A wealth of information is available in scientific journals, newspapers, and other sources, enabling us to reconstruct the storm timeline. This shows that a series of major coronal mass ejections (CMEs) bombarded Earth in May 1921. The first pair may have prepared the way for latter intense activity, clearing density from the region between Sun and Earth, and energizing Earth's magnetosphere. Thus, a subsequent CME could travel more quickly and drive even more energy into the already active magnetosphere. This CME arrived late on 14 May, driving very intense activity early on 15 May, and leading to the spectacular technological effects. However, some effects, attributed at the time to space weather, were probably coincidental with the storm, and due to more prosaic faults. The timeline of the 1921 event, including the confusion caused by prosaic faults, can be used to construct scenarios for use today by those emergency managers planning how to reduce the adverse impacts of future space weather events.

1. Introduction

Over the past decade the public perception of space weather has changed markedly so that it is now considered a major societal risk alongside other natural hazards including pandemic disease, extremes of temperature, coastal and river flooding, earthquakes, and volcanic activity (OECD, 2018). As a result of this step change in public perception, improved understanding of severe space weather, and its impacts, is now a vital element in the scientific evidence sought by policy-makers responsible for societal resilience (Hapgood, 2018). Those policy-makers require information on both the likelihood, and the adverse impacts, of severe space weather, just as they do for other natural hazards. Only then can they integrate space weather into wider plans to ensure societal resilience against the whole range of natural hazards (OECD, 2018).

Many policy-makers recognize that the adverse impacts of severe space weather arise mainly from the disruption of engineered systems (Cannon et al., 2013), especially the disruption of critical infrastructures that now sustain everyday life and economic activity. They need evidence that enables them to assess the following:

1. the extent to which disruption caused by space weather can be mitigated by generic measures such as those to restore electric power after problems with transmission networks;
2. where that mitigation needs to be underpinned by measures specific to space weather, most obviously the provision of forecasts of adverse space weather; and
3. the cost-effectiveness of both generic and specific measures.

A key element in this evidence is the likely timelines of extreme space weather events. Such knowledge enables us to build scenarios that give insights into the spatial and temporal distribution of adverse impacts, and into the information that will be available to enable timely decision-making before, during and after an extreme event. They are also vital for exercises to test mitigation plans and to train key personnel in government and industry (Cabinet Office, 2015; Krausmann et al., 2016). Scenarios are also critical inputs for realistic studies on the socio-economic impact of space weather (Eastwood et al., 2018; Oughton et al., 2018).

This study addresses one route to scenario development, namely, a review of previous severe space weather events, and specifically focuses on one outstanding case, the great storm of 13-16 May 1921, and particularly the very intense activity on 14/15 May. It complements studies that have developed scenarios around previous severe events of 1859, 1989, and 2003 (Eastwood et al., 2018), as well as studies that have simulated severe events using the very fast CME of July 2012 as a basis for that simulation (Baker et al., 2013; Ngwira et al., 2013). This complementarity is important; we must recognize that there will be differences between individual severe space weather events, so the development of mitigation plans and exercises must be informed by a range of scenarios.

The May 1921 storm is a valuable contribution to this range because we can review the wealth of information available from scientific and engineering records, and from newspaper reports. As we will discuss below, this information includes a rich set of geomagnetic activity reports from observatories all over the world, and much evidence of adverse impacts due to geomagnetically induced currents (GICs) in electrically grounded infrastructures, primarily telecommunications systems such as telegraph lines and transoceanic cables. Those GIC impacts are a valuable proxy for today's headline risk from space weather, namely, the risk of disruption in electricity transmission networks (Cannon et al., 2013; Krausmann et al., 2016).

But first, we must present detailed information about the May 1921 storm. In section 2, we outline key background including (a) how geomagnetic variations were monitored in 1921 and particularly features that affect data quality, (b) the time systems in use in 1921, and (c) how we calculate contextual information such as the magnetic latitudes, times of sunrise, sunset, and twilight at various observing sites. In section 3 we present and discuss the timeline of geomagnetic activity during the very intense activity on 14/15 May and the precursor activity that may have preconditioned the heliosphere and the magnetosphere to generate that very intense activity. Moving to section 4, we report and discuss the timeline and spatial location of impacts observed during the very intense activity. We divide those impacts into three classes: (a) GIC impacts on wired telecommunications, (b) auroral reports as a visual indicator of the changing level of storm activity, and finally (c) impacts on radio propagation. The aurora is included in these impacts because it provides insights on temporal and spatial variations that complement the other impacts. Section 5 discusses storm effects and impacts that occurred after the very intense activity, not least the further strong geomagnetic activity that occurred on 16 May. This is included to give a complete picture of the storm, completeness that is important for the building of scenarios. In section 6 we bring together all the information presented in the previous three sections and discuss how this can be integrated into a consistent physical picture, one that can support a well-rounded scenario. Finally, in section 7 we summarize our results and discuss how they may be developed further through modeling and through further exploration of relevant records from 1921.

2. Materials and Methods

2.1. Time Scales Used in This Paper

The information presented in this paper is gleaned from a wide range of scientific and popular reports on the May 1921 storm, and with an especial focus on reports that give the time of day when effects were observed, not just the date. However, time standards in 1921 were more subject to local variation than they are today. So care has been taken to check the time standards used in each report.

Fortunately, by 1921, the international scientific community had long grasped the importance of time standards. So many scientific reports of that era already used Greenwich Mean Time (GMT) as an international standard, and most other scientific reports provided information on how to convert their local time to GMT, for example, reports from the U.S. East Coast used standard time for a longitude of 75° west (i.e., the basis of modern Eastern Standard Time). It is more tricky to check time standards used in popular reports, such as newspaper reports. In particular, care is needed to check on use of daylight saving time, a system that was in its infancy in 1921 and subject to considerable local variation (as we will note below when needed).

One feature in scientific time standards used in 1921 is potentially confusing to the modern eye, namely, that astronomers sometimes recorded GMT using a 24-hr clock starting at noon at zero longitude, and sometimes using a clock starting at midnight. This potential ambiguity led to other terms also being used, including some found in the auroral records used in this paper: Greenwich Mean Astronomical Time (GMAT) for times starting at noon, and Greenwich Civil Time (GCT) for times starting at midnight (Allen, 2019). Thus, there is potential for confusion in the times of auroral observations; but, in practice, these cases are easy to resolve given that such observations must have been made during hours of darkness.

In this paper, we will present times as GMT since that was the international standard in use at the time of the storm. This is broadly similar to Universal Time, which was introduced from 1928 onward in order to leave behind the ambiguous usage of GMT (IAU, 1928). However, GMT should not be regarded as similar to Coordinated Universal Time, as this latter standard is well defined only from 1960 (Allen, 2019). We will also outline where and how we converted local times to GMT (e.g., see notes in Tables 2 and 3).

2.2. Magnetometer Measurements

In 1921 there was already a significant global network of magnetic observatories, with strong collaboration between the scientists working at those observatories. That network had grown during the nineteenth century following Gauss' development of techniques to measure the vector components of the geomagnetic field (see Nevanlinna, 1997, and references therein). The measurements of 1921 exploited the same basic principle, namely, the use of suspended magnets to detect changes in geomagnetic field components. In early magnetometers, the deflection of the magnets was recorded manually, but, as noted by Brooke and Airy (1847a, 1847b), it was quickly realized that photographic recording of the deflection would enable continuous measurements of temporal variations in the geomagnetic field. In these "variometers," the deflection of each magnet was detected by reflecting a beam of light from a mirror attached to the magnet, and measuring the consequent deflection of the beam. The basic principle of such measurements was to wrap photographic paper round a slowly rotating drum that had its axis parallel to the direction of movement of the optical beam from the suspended magnet. Thus, the time series of each geomagnetic field component would be imprinted on the photographic paper. This basic technique for variometer measurements proved very durable; it was refined over the years, as discussed in section 2.9 of Chapman and Bartels (1940), and continued in widespread use until the advent of modern digital measurements. However, the technique is subject to two constraints that are important to the interpretation of the 1921 geomagnetic measurements: (a) extreme geomagnetic variations can deflect the light beam beyond the edges of the photographic paper on the recording drum and (b) observations must be periodically interrupted for a few minutes to replace that photographic paper. We will see examples of both constraints in the data presented in this paper, but also examples of how skilled observers could mitigate the first constraint through by using additional calibrated magnets to bring the light beam back on the photographic paper.

Most of the discussion in this paper focuses on the observed variations in the horizontal component of the geomagnetic field. This was widely abbreviated in the literature to a single letter acronym of H, and we will use that same acronym in this paper. In a few cases, notably the magnetometer at Greenwich, the northward component of the geomagnetic field was measured, rather than H (Newton, 1948). The acronym N was, and is, used in that case. In addition, the acronyms D and Z are used, respectively, for declination (the angle between H and N) and for the vertical component of the geomagnetic field.

2.3. Magnetic Latitudes

The magnetic latitudes of the observing sites cited in this paper are magnetic dipole latitudes calculated by the author using a geomagnetic dipole orientation appropriate to May 1921. That orientation was derived from the International Geomagnetic Reference Field (IGRF) model (Thébault et al., 2015), and specifically

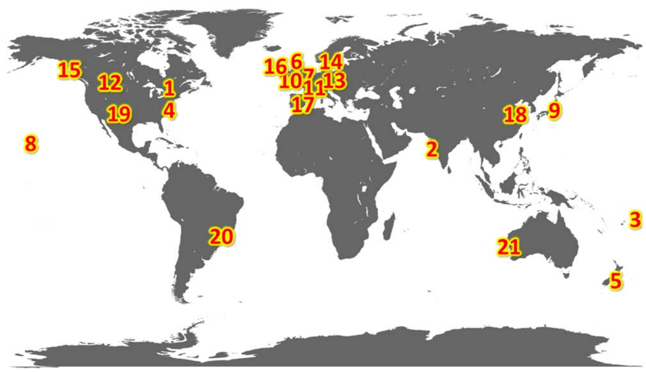

Figure 1. Locations of the geomagnetic observatories whose published observations have been have been used in this paper and that are summarized in Table 1. Numbers refer to entries in that table. Background world map sourced from https://commons.wikimedia.org/wiki/File:World_map_blank_without_borders.svg.

from the definitive IGRF models for 1920 and 1925, interpolated to year 1921.4. The derivation of dipole orientation from IGRF parameters follows the method described by Hapgood (1992), with the correction given in Hapgood (1997).

2.4. Twilight and Sunset Times

To assist with the interpretation of auroral observations, and of radio signal propagation, the Jet Propulsion Laboratory Horizons web tool (currently available on https://ssd.jpl.nasa.gov/horizons.cgi) was used to calculate end and start times of twilight (both nautical and astronomical), and times of sunset and sunrise, where these times are cited throughout the paper.

3. Geomagnetic Observations of the Storm

The scientific literature contains a wealth of reports of the geomagnetic variations observed during the storm. This paper uses information gathered from reports published by the observatories whose locations are shown in Figure 1 and whose reports are summarized in Table 1.

These reports show that severe geomagnetic activity occurred around the time that a large active region (Mount Wilson region 1842) crossed the central meridian of the Sun on 14 May (Cortie, 1921a; Mount Wilson, 1921; Royal Greenwich Observatory, 1955). Within that activity, there are two features that we will explore in this section: (a) a main focus on the period of very intense activity between 01:00 and 08:00 GMT on 15 May following a sudden commencement (SC) late on 14 May, complemented by (b) a secondary focus on the earlier period of intense activity following two SCs on 13 May. We highlight these because of the notable space weather impacts (major damage to property) associated with the very intense activity and the possible role of the earlier activity in preconditioning the heliosphere and magnetosphere to generate the very intense activity.

For avoidance of doubt, please note that no attempt has been made to survey original photographic records from these magnetometer stations. That would be a major undertaking that is beyond the scope of this study, in terms of both resources and specialist skills. Instead, this paper has exploited material published in the scientific literature, including high-quality calibrated reproductions of magnetometer traces from several stations.

3.1. Precursor Activity, 13/14 May

A large SC occurred around 13:10 GMT on 13 May and was followed by a second smaller SC at 19:24 (see Figure 2a). These were the first two of four substantial SCs observed during the storm **(**Observatori de l'Ebre**,** 2019). These SCs suggest that the Earth was bombarded by a series of coronal mass ejections during the storm.

The first SC was particularly striking, with amplitudes above 100 nT being observed across the dayside, and above 70 nT on the nightside. But, as summarized in Table 1 and Figure 2a, substantial activity started only around the time of the second SC, with intense activity being reported in Europe between 21:00 and 22:00. Magnetometer observations from Rude Skov, 20 km north of Copenhagen (Stenquist, 1925), show a large spike-like depression (~1,300 nT) in H at 21:24, together with marked changes in D and Z. Following the Biot-Savart law for magnetic fields generated by electric currents (Bleaney & Bleaney, 1965), and specifically the consequent right-hand rule for the orientation of those fields, this depression suggests the presence of a westward electrojet around 56° magnetic latitude, with some complex currents embedded in that part of the electrojet over Denmark and southern Sweden. Further evidence for the presence of the electrojet at these latitudes comes from the Greenwich magnetometer observations (Dyson, 1924), which show a marked upward perturbation (~200 nT) at this time. Using the right-hand rule again, this is consistent with a westward electrojet just north of Greenwich (54° magnetic latitude in 1921). Further evidence of the intense activity over Europe comes from observations of bright aurora high in sky between 21:00 and 22:00 as seen from England, France, Germany, Sweden, and Wales as listed in Table 3. This activity also disrupted of telecommunications systems across Denmark, southern and central Sweden as shown in Table 2. Global activity

10.1029/2019SW002195

Table 1
Summary of Geomagnetic Effects Recorded on 13 to 15 May at the Observatories Used in This Study

N	Station	Latitude (°N), Longitude (°E)	Observed activity at, and following, large SC on 13 May	Observed activity during intense storm period after 22:00 on 14 May	References	Time used in reference
1	Agincourt, Canada	43.8, 280.7	Major disturbance. Range of 856 in H.	Major disturbance. Range of 1118 in H.	Jackson (1921)	no timed data given
2	Alibag, India	18.6, 72.9	SC of 130 nT at 13:11.	230 nT SC at 22:15. H off chart from 03:25 to 05:50 next day despite use of deflector magnet	Chinmayanandam (1921)	GMT+4hr 51 m "Bombay time"
3	Apia, Samoa	-13.8, 188.2	SC of 70 nT at 13:09. Strong activity from ~19:15. Range in H of 210 nT, minimum H at 05:53 next day	Intense activity between 22:13 and 10:30 next day. Range in H ~ 920 nT and in Z 75 nT. Minimum H at 05:30.	Angenheister and Westland (1921a, 1921b)	GMT
4	Cheltenham, USA	38.7, 283.2	SC at 13:09 on 13 May. Great intensity from 19:00 until 10:00 next day.	Intense activity between 22:00 and 09:00 next day. H off chart at times. Range in H ~ 800 nT and in Z 1000 nT	Hartnell (1921)	GMT-5hr
5	Christchurch, NZ	-43.5, 172.6	SC of 120 nT at 13:08.	Intense activity from 22:00. Oscillations in H were too rapid to be recorded from 22:00 to 24:00, and from 03:00 to 05:00 next day. Range >750 nT in H. H off chart between 03:00 and 05:00, also between 06:15 and 07:30.	Skey (1921)	GMT+11hr 30m in text, GMT on plots
6	Eskdalemuir, UK	55.3, 356.8	SC at 13:02 with large amplitude such that N did not register on the photographic paper record. Intense activity between 20:00 and 22:00 with range >500 nT in N. N off chart at 21:24.	Intense activity after 23:00, and particularly between 01:00 and 06:00 next day, when there were at least 12 events when Z rapidly moved between the limits of the instrument. Strongest was between 02:40 and 02:44 with a rate of change of 138 nT/min in Z.	Mitchell (1921)	GMT
7	Greenwich, UK	51.5, 0	SC of 120 nT at 13:10. Strong activity from 19:20, in particular 21:30-22:20. Range of >400 nT in N, minimum N ~22:00. Marked upward perturbation (~200 nT) at 21:30-22:20 suggests westward electrojet near to, but north of, Greenwich.	Intense activity between 22:00 and 08:00 next day. N off chart between 02:00 and 02:30, also 03:00 and 06:30; Z off chart between 00:30 and 10:30. Range > 700 nT in N and > 450 nT in Z.	Newton (1948) and Dyson (1924)	GMT
8	Honolulu, USA	21.3, 202	SC of 130 nT at 13:10. Strong activity from 19:00 to 08:00 next day. Range in H of ~320 nT, minimum H at 05:55.	Sharp onset of intense activity at 22:15. H off chart after 03:30 next day.	Kappenman (2006)	GMT
9	Kakioka, Japan	36.2, 140.2	SC at 13:11 GMT.	Intense activity from 22:39. H off chart at times. Range ≥ 1000 nT in H and 337 nT in Z	Kunitomi (1921)	GMT in text, GMT+9hr in table
10	Kew, UK	51.5, 359.7	SC of 120 nT at 13:10, followed by only moderate until nearly 20:00, then stronger activity until 08:00 next day.	Intense activity after 2200, especially between 00:00 and 08:00 next day. H off chart from 03:00 to 07:30. Range > 650 nT in H and ~1,500 nT in Z. Starting 03:53, Z rose by 1,400 nT in 13 min.	Chree (1921a)	GMT
11	Lyon, France	45.7, 4.8		Marked oscillations in D (>0.5°) at 01:20 and 02:50 next day. D off chart in negative direction 03:30 to 04:40, 06:00 to 06:50 and 07:10 to 07:50. Large positive excursion in D at 05:25.	Fouche (1921)	GMT

Table 1
(continued)

N	Station	Latitude (°N), Longitude (°E)	Observed activity at, and following, large SC on 13 May	Observed activity during intense storm period after 22:00 on 14 May	References	Time used in reference
12	Meanook, Canada	54.6, 246.7	Very disturbed, report notes that “It is impossible to approximate the amplitudes for Meanook”	as for 13 May SC	Jackson (1921)	no timed data given
13	Potsdam (Seddin), Germany	52.3, 13		SC of ~150 nT at 22:10, followed by intense activity until 08:00 next day, particularly between 03:00 and 06:00. Range ≥1,500 nT in H and at least 700 nT in Z. One brief spike extends range of Z to 1,000 nT	Figure 34a of Chapman and Bartels (1940)	GMT
14	Rude Skov (Birkeröd), Denmark	55.8.12.5	SC of 260 nT at 13:11. Significant activity from 19:00 to 06:00 next day. Dominant feature is sharp spike-like variation at 21:24, with depression of 1,300 nT in H, also marked variations in D and in Z. Range of 1,300 nT in H and 900 nT in Z.	Sharp onset of intense activity from 22:10, continuing to 08:00 next day. Clear depressions of H around 01:00 and 2:00. H off chart between 03:00 and 06:00. Another depression in H around 07:00. Range of >1,450 nT in H and >1,150 nT in Z.	Stenquist (1925)	GMT+1hr
15	Sitka, USA	57.1, 224.7	Short-lived bipolar signature (±30 nT in H) at 13:11. Overlaps with longer-lived feature in D. Strong activity from 19:00 onward. Range in H of >1,200 nT, maximum H at ~05:40 next day, followed by minimum at ~12:25 and secondary minimum around 15:30.	Sharp onset of intense activity after 22:00 H off chart between 03:00 and 07:00 next day.	Kappenman (2006)	GMT
16	Stonyhurst, UK	53.8, 357.5	SC at 13:12. Significant activity between 21:00 and 24:00.	Intense activity between 22:25 and 07:30 next day. H lost due to instrumental problems. Z off chart from 00:24 to 09:12. Range > 461 nT in Z.	Cortie (1921b)	GMT
17	Tortosa, Spain	40.8, 0.5	SC at 13:10. Strong activity from 19:18	H off chart from 03:00 to 11:00 next day. Range ≥ 660 nT in H	Rodes (1921) and Cortie (1921a)	GMT
18	Tsingtau (Qingdao), China	36.1, 120.3	SC at 13:11	H off chart from 03:00 to 09:00 next day. Range ≥600 nT in H and ~160 nT in Z	Irumata (1921)	GMT
19	Tucson, USA	32.3, 249.2	SC of 80 nT at 13:06. Strong activity from 18:30 to 07:00 next day. Range in H of ~340 nT, minimum H at 22:00.	Sharp onset of intense activity at 22:00. H off chart after 03:00 next day.	Kappenman (2006)	GMT
20	Vassouras, Brazil	-22.4, 316.4	SC of 126 at 13:12. Strong activity from 19:21 to 09:15 next day.	Intense activity from 22:18 to 12:00 next day, H off chart at times on both recording devices. Range was 1008 nT in H and 112 nT in Z	Lemos (1921)	GMT
21	Watheroo, Australia	-30.3, 115.9	SC of 70 nT at 13:09. Strong activity from 19:17 to 16:00 next day.	SC of 40 nT at 22:15. H off chart from 23:30	Parkinson (1921)	GMT+8hr

Note. See Text note S3 for details on the derivation of SC sizes.
Abbreviation: SC, sudden commencement.

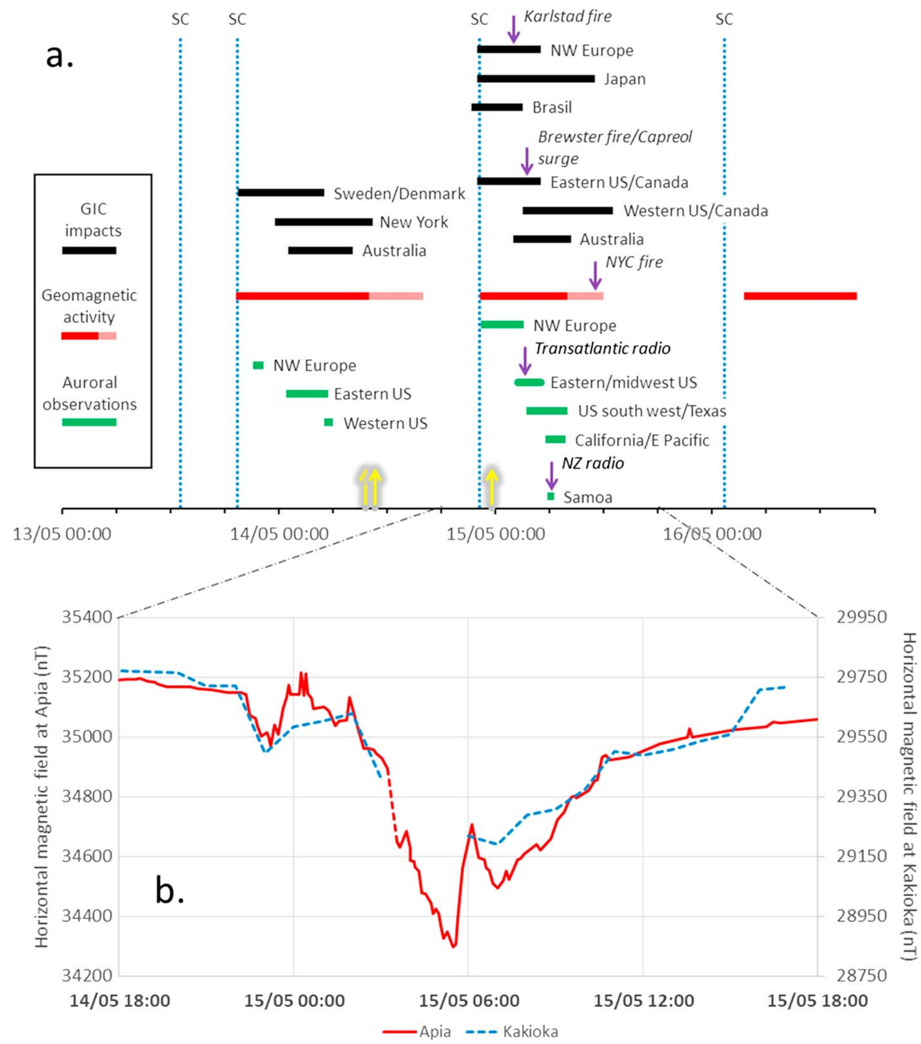

Figure 2. (a) Timeline summarizing the durations and locations of the geomagnetically induced current (GIC) impacts (black bars) and auroral observations (green) on 13-15 May. The red bars mark the duration of the geomagnetic activity: those with a lighter shade of red indicating moderate activity following the more intense activity indicated by the bolder shade of red. To set this activity in context, the duration of the subsequent geomagnetic activity on 16 May is also shown, as are the times of sudden commencement (SCs; vertical blue dashed lines). The yellow arrows at the bottom of panel indicate when the solar active region causing the storm was facing the Earth—each arrow marks the central meridian crossing time of one of the three large umbrae in the active region (Tamm, 1922). The five magenta arrows indicate the times of key GIC and radio system incidents discussed in the text below. (b) The horizontal component of the geomagnetic field as measured as Apia and Kakioka before, during and after the very intense geomagnetic activity on 15 May 1921. Apia data traced from a digital copy of Plate II of Angenheister and Westland (1921a), and Kakioka data taken from table H of Kunitomi (1921). The dashed section of the Apia record replicates a similar but unexplained feature in the published data, perhaps replacement of the photographic paper used to record the variation of H.

continued well into the 14th with equatorial magnetometers (Apia and Honolulu) reporting a depression in H of 150 to 200 nT with the lowest values reported around 06:00 on the 14th (Angenheister & Westland, 1921a; Kappenman, 2006). There were also extensive observations of aurora across the United States and reports of telegraph system disruption from Australia and the United States (see Tables 2 and 3, also Figure 2a).

A detailed analysis of the first SC on 13 May is given in the supporting information. It suggests that this large SC was caused by impact of a CME that had been launched from the Sun some 20 to 27 hr previously, a launch period that is consistent with reports of strong solar activity, as noted by Lundstedt et al. (2015).

10.1029/2019SW002195

Table 2
Examples of Disruptions to Telegraph and Telephone Systems Around the World During 13 to 15 May

Country	Start time	End time	Impacts	Reference	Notes
Norway	13 May 1921	16 May 1921	No specific times, but the Fouche reference includes letter from Carl Størmer noting the extreme violence of currents in the Norwegian telegraph systems leading to breaks and sparks.	Fouche et al. (1921)	
UK & Ireland	13 May 1921 13:00	17 May 1921 04:00	Large Earth currents observed in telegraph systems across England, Scotland and Ireland	Chree (1921)	
United States	13 May 1921 15:00	13 May 1921 21:00	Problems with telegraph systems at Rock Island, Illinois	Rock Island Argus (1921a)	Rock Island on Central Standard Time, GMT - 6 hr. See Text S1
Sweden	13 May 1921 19:00	14 May 1921 05:00	Extremely powerful earth currents experienced in practically all telegraph and telephone circuits south of a line passing through Östersund and Söderhamn, also “In many cases, security devices were destroyed.”	Stenquist (1925)	Take night as 8 p.m. to 6 a.m. local. Sweden on CET, no DST in 1921, so GMT+1hr
New Zealand	13 May 1921 20:30	16 May 1921 14:00	Extensive problems on telegraph lines with earth currents driving voltages up to 60 V, and often showing wide range of fluctuations. Problems could be mitigated by using wired return connection, rather than earth return.	Gibbs (1921)	NZST = GMT +11 hr 30 min in 1921
Denmark	13 May 1921 21:00	14 May 1921 01:00	Telephone lines from Copenhagen to Göteborg and Stockholm unusable	Sheffield Independent (1921)	Denmark on CET, no DST in 1921.
Sweden	13 May 1921 21:00	14 May 1921 07:30	Telephone lines between Göteborg and Stockholm unusable	Sheffield Independent (1921)	Sweden on CET, no DST in 1921.
United States	14 May 1921 00:00	14 May 1921 10:00	Telegraph services in New York sluggish due to earth currents.	NYT (1921e)	Take night as 8 p.m. to 6 a.m. local time, DST in operation, so local time = GMT-4 hr.
Australia	14 May 1921 01:00	14 May 1921 02:30	Earth currents up to 15 mA on lines in South Australia.	Parkinson (1921)	Report comes from Perth where local time = GMT + 8 hr
Australia	14 May 1921 01:00	14 May 1921 08:10	Earth currents up to 50 mA measured on telegraph lines in Western Australia. Alternating with period around 20 s.	Parkinson (1921)	Local time = GMT + 8 hr
France	14 May 1921 19:00	15 May 1921 05:00	Telegraph systems in Paris unable to receive messages from rest of Europe, or from the United States, during the night of 14/15 May.	Fouche et al. (1921) Matin (1921)	Take night as 8 p.m. to 6 a.m. local time. DST in operation so local time = GMT + 1 hr in 1921
Japan	14 May 1921 21:00	15 May 1921 11:00	Telegraphic communications said to have been bad at many parts of Japan on the day of main perturbation of the magnetic storm.	Kunitomi (1921)	Take day to be 6 a.m. to 8 p.m. local time. No DST in 1921, so local time-GMT+9 hr
Brazil	14 May 1921 21:20	15 May 1921 03:00	Strong Earth currents, and telegraph disruption, on routes north and south of Sao Paulo (to Uberabinha and Porto Alegre, respectively), also on coastal routes north of Rio (e.g., Rio to Vitoria, Bahia-Ilheus), but only weak currents (and no telegraph disruption) observed on direct routes between Sao Paulo and Rio	Lemos (1921)	NB Sao Paulo (& Brazil) was on GMT-3 hr in 1921, no DST. Note that these reports appear to end at local midnight.
United States	14 May 1921 22:00	15 May 1921 06:00	Telegraph disruption in Omaha, Nebraska. Western Union and Associated Press (AP) services	Omaha Daily Bee (1921)	

10.1029/2019SW002195

Table 2
(continued)

Country	Start time	End time	Impacts	Reference	Notes
			disrupted from 16:00 local time, postal wires to Chicago down from 21:00 local time, AP services almost unusable after 22:00 local time and for much of night		Local time = GMT-6 hr. A newspaper search shows no mention of DST in Omaha between 1917 and 1925.
United States	14 May 1921 23:00	15 May 1921 06:00	Near total cutoff of telegraph services in Rock Island, Illinois, starting at 17:00 local time, and continuing much of the evening.	Rock Island Argus (1921a)	Rock Island on Central Standard Time, GMT-6 hr. See Text S1. Assume it continues until local midnight
Sweden	15 May 1921 00:00	15 May 1921 06:00	Earth current measurements at Göteborg on line to Stockholm show GIC of 1.1 amp at 00:20. The hourly average geoelectric fields derived from these measurements were >100 mV/km between 02:00 and 06:00.	Stenquist (1925)	Sweden on CET, no DST in 1921, so GMT+1 hr
Sweden	15 May 1921 00:20	15 May 1921 05:00	Disruption of telegraph and telephone lines at main exchange in Stockholm with "a very loud song was heard in every line."	Stenquist (1925)	Sweden on CET, no DST in 1921, so GMT+1 hr
United States	15 May 1921 00:30	15 May 1921 06:00	Disruption of telegraph services at Columbia, Missouri. Problems started 18:30 local time, all communications lost from 19:00. No specific end time but clearly continued for much of that evening. Some damage to equipment: platinum tips on sending machines ("bugs") melted, some damage to insulation. No impact on local phone service.	Columbia Evening Missourian (1921)	A newspaper search shows no evidence for DST being used in Columbia. So local time = GMT-6 hr. Assume end time of local midnight.
Sweden	15 May 1921 01:00	15 May 1921 02:00	Catastrophic damage at the telegraph and telephone station at Karlstad, initially disruption of equipment and some smoke, but later a fire that destroyed the exchange. Analysis by Stenquist indicates that the damage required geoelectric fields between 6 and 20 V/km.	Karsberg et al. (1959) Stenquist (1925)	Sweden on CET, no DST in 1921, so GMT+1 hr
Sweden	15 May 1921 01:00	15 May 1921 02:00	Minor fire at the telegraph and telephone station of Ånge. Initial problems were similar to those at Karlstad, but precautionary measures averted catastrophe.	Stenquist (1925)	Sweden on CET, no DST in 1921, so GMT+1hr
United States	15 May 1921 01:15	15 May 1921 02:15	Telegraph services to Atlanta blocked by earth currents. Voltages of 350 to 400 V reported. No impact on phones as these lacked earth connections.	Atlanta Constitution (1921)	Atlanta on DST, local time = GMT-4 hr
Australia	15 May 1921 02:00	15 May 1921 08:20	Significant Earth currents on telegraph lines in Western Australia.	Parkinson (1921)	Local time = GMT + 8 hr
United States	15 May 1921 02:00	15 May 1921 17:00	Substantial damage to telegraph and telephone systems along the Boston and Albany Railroad, especially between Springfield and Albany. Voltages of 400 V measured on some lines in Boston.	Springfield Republican (1921)	Problems on B&A from 22:00 to 13:00 local time, GMT-4 hr

10.1029/2019SW002195

Table 2
(continued)

Country	Start time	End time	Impacts	Reference	Notes
Canada	15 May 1921 02:15	15 May 1921 05:00	Reports current and voltage measurements on 1,200-km telegraph line that runs east- west from Montreal via Capreol to Port Arthur (now Thunder Bay). Currents up to 0.2 amps measured at Capreol between 21:15 and 22:30 local time. Measurements were abandoned at 22:30 when a surge of higher currents endangered equipment, necessitating disconnection of lines to protect equipment. These large effects continued past local midnight.	Telegraph and Telephone Age (1921a)	Ontario on GMT-5 hr. Switch to DST in Ontario was scheduled for 02:00 local time on 15 May, that is, 07:00 GMT.
United States	15 May 1921 02:30	15 May 1921 05:00	Period of greatest disturbance on telegraph systems across eastern United States. especially New York and Chicago. Earth currents causes voltages up to 1,000 V. NB Auroral arc overhead of NY at this time - see "curtain flapping in the wind" in NYT.	Lyman (1921), NYT (1921a), NYT (1921c), and LAT(1921)	Chicago on DST GMT-5 hr, NY on DST GMT-4 hr
United States	15 May 1921 02:30	15 May 1921 03:00	Report from Hartford, Kentucky, notes widespread disruption of telegraph and long-distance phone services - largely unusable during much of the time that aurora was visible (peak was 21:30 to 22:00 local time). Also notes that railway (sic) trains were forced to suspend operations for a short time during that night, due to interference with electrical devices for signals	Hartford Republican (1921)	No DST in Hartford, so local time = GMT-5 hr. News item in Hartford Herald (1921) indicates that DST was adopted in Louisville, but not other areas of Kentucky such as Hartford
United States	15 May 1921 03:00	15 May 1921 04:00	Railroad station at Brewster in New York state destroyed by fire attributed to strong earth currents in telegraph wires.	Brewster Standard (1921a)	Brewster on DST, same as Railroad, GMT-4 hr. See Text S1.
United States	15 May 1921 03:00	15 May 1921 07:00	Disruption of telegraph systems in Phoenix, Arizona from 20:00 local time. Telegraph line to Denver out of action during night with brief recovery around 22:30 local time.	Arizona Republican (1921a)	Phoenix on Mountain Standard Time, GMT-7 hrs. See Text S1.
United States	15 May 1921 03:00	15 May 1921 13:00	Extensive disruption of telegraph systems in western United States, including loss of all services to/from Helena (Montana), and on all routes to Alaska. But severe impacts over wider area including Denver, Salt Lake City, San Francisco, Seattle and Spokane, peaking just before 07:00 on the 15th (midnight in Helena)	Lyman (1921): Independent-Record (1921)	Helena out all night: take as 8 p.m. to 6 a.m. local time, GMT-7 hr

Note. See text note S1 for further discussion of event times in Karlstad, Brewster, Rock Island, and Phoenix and time zone nomenclature.

10.1029/2019SW002195

Table 3
Examples of Auroral Observations Made Around the World on 13 to 15 May

Country	Start time (GMT)	End time (GMT)	Observations	Reference	Notes
Germany	13 May 1921 21:10	13 May 1921 22:20	Observation of coronal aurora from Bremen in northern Germany between 22:10 and 23:20 (time zone unspecified). Brightest at 22:30.	Wilkens and Emde (1921)	Nautical Twilight (NT) ended 20:55 GMT. Assume observations recorded in MEZ (Mitteleuropäische Zeit, GMT+1 hr) as in adjacent article on observations from Breslau—see 14 May 1921 00:20 below
UK	13 May1921 21:25	14 May 1921 02:25	Aurora seen at the zenith from Cambridge	Chree (1921)	NT ended 21:25, started 02:25 GMT
UK	13 May 1921 21:25	13 May 1921 22:20	Aurora seen from Pontypridd in Wales and from several sites in eastern England	Hudson (1921) Burns (1921)	Observations recorded in GMT.
France	13 May 1921 21:40	13 May 1921 21:50	Aurora seen from Fay-Sarthe in the Loire valley between 22:40 and 22:50 local time (“heure légale”).	Fouche et al. (1921)	Local time = GMT + 1 hr
Sweden	13 May 1921 21:30	13 May 1921 22:00	Aurora seen widely across southern Sweden between 22:30 and 23:00 CET.	Stenquist (1925)	Stenquist's report consistently uses CET (= GMT + 1 hr) for all times.
United States	14 May 1921 01:15	14 May 1921 05:00	Brilliant aurora seen from Manning, South Carolina (45° magnetic latitude) with rays reaching the zenith	Manning Times (1921)	Eastern time zone, GMT - 5 hr, Assume display seen between end of NT (01:15 GMT/20:15 local) and local midnight (05:00 GMT). A newspaper search shows no mention of DST in Manning after 1919.
UK	14 May 1921 22:23	15 May 1921 02:15	Aurora observed from Walton in Surrey, also sites in East Anglia. Most intense around 02:00 GMT	Burns (1921)	NT ended at Walton 21:20, started 02:35. Observations recorded in GMT.
United States	14 May 1921 05:30		Bright aurora seen from Salmon, Idaho, about 22:30 local time on 13 May	Idaho Recorder (1921)	Mountain time zone, GMT - 7 hr. NT ended 04:15 GMT
France	15 May 1921 00:20	15 May 1921 03:05	Aurora observed by Bernard Lyot and colleagues at Meudon between moonset and first light. Lyot notes three maxima of auroral intensity at 01:14, 02:10 and 03:05. The second maximum was most intense, obscuring some second magnitude stars and providing enough light to read watches and make notes. Intense maximum around 02:00 confirmed by another French observer (Robert Mariette) viewing the aurora from near Le Havre.	Fouche et al. (1921) and also Lyot (1921)	NT started 02:45, solar depression was -9.5° at 3:05. Lyot explicitly notes that his observations are timed in GMT (“T.m.de Gr.”)
Germany	15 May 1921 00:20	15 May 1921 01:30	Magnificent aurora seen from Breslau (now Wrocław) by astronomer returning home from observatory	Wilkens and Emde (1921)	Astronomical twilight started 00:10 GMT, NT started 01:30. Wilkens noted that his observations were timed in MEZ (Mitteleuropäische Zeit, GMT+1 hr)
United States	15 May 1921 02:30	15 May 1921 03:00	Bright aurora observed between 21:30 and 22:00 local time on May 14 from Hartford, Kentucky	Hartford Republican (1921)	No DST in Hartford, so local time = GMT-5 hr. News item in Hartford Herald (1921) indicates that DST was adopted in Louisville, but not other areas of Kentucky such as Hartford
United States	15 May 1921 02:30	15 May 1921 05:00	Auroral arc overhead of New York at this time—see “curtain flapping in the wind” in NYT.	NYT (1921a)	New York on DST, local time = GMT-4 hr (eastern daylight time)
United States	15 May 1921 02:00	15 May 1921 03:00		Omaha Daily Bee (1921)	NT ended 02:45. Local time = GMT - 6 hr. A newspaper search shows no

10.1029/2019SW002195

Table 3
(continued)

Country	Start time (GMT)	End time (GMT)	Observations	Reference	Notes
			Aurora seen from Omaha soon after sunset (19:30 local time), bright coronal display around 21:00 local time		mention of DST in Omaha between 1917 and 1925.
United States	15 May 1921 02:00	15 May 1921 05:00	Spectacular aurora described by a Weather Bureau observer at Drexel Aerological Station, 30 km north west of Omaha, Nebraska, starting around 21:00 local time, and very intense from 21:40 through to midnight, some activity continuing through to daylight.	Lyman (1921)	NT ended 02:45, started 10:00. Observations may be reported as DST (GMT-5 hr). A search of weather bureau records shows that "some observers take observations on daylight saving time." This would make this report consistent with separate newspaper report from Omaha
United States	15 May 1921 03:00		Spectacular auroral display visible from Phoenix, Arizona, from about 20:00 local time until late.	Arizona Republican (1921a)	Phoenix on Mountain Standard Time, GMT - 7 hr. See Text S1.
United States	15 May 1921 03:25	15 May 1921 03:30	Brilliant aurora observed from Rock Island, Illinois—at its greatest intensity between 21:25 and 21:30 local time on 14 May, according to observer from local weather bureau.	Rock Island Argus (1921a)	Rock Island on Central Standard Time, GMT - 6 hr. See Text S1.
United States	15 May 1921 03:25	15 May 1921 08:00	Bright aurora seen from Lowell Observatory in northern Arizona with strong activity around 21:00 and 23:00 local time, with "more or less subdued intensity duringabout an hour" in between these two bursts of activity. Thereafter the display faded to glow in north by 01:00 next day. Also third party report of another display later that same night.	Russell et al. (1921)	NT ended 03:25, started 11:20. Observations reported in Mountain Time (GMT-7 hr)
United States	15 May 1921 03:30	15 May 1921 04:30	Report in Dallas Times of bright aurora seen during this hour (09:30-10:30 local) from San Antonio. Also notes disruption of radio systems at Fort Sam Houston	Lyman (1921)	NT ended 02:15. Observations reported in local time (GMT-6 hr)
United States	15 May 1921 03:30	15 May 1921 10:30	Bright aurora observed from Tucson in southern Arizona from 20:30 local time to daylight next day. Notes that it became less intense at 22:30, then showed renewed activity a short time later. The display had diminished by 01:00, but there was significant activity on northern horizon at 03:30.	Douglass (1921)	NT ended 03:10, started 11:30. Observations reported in local time (GMT-7 hr)
United States	15 May 1921 03:45	15 May 1921 05:00	Observations from Prescott, Arizona, by retired senior and distinguished astronomer, Milton Updegraff. Aurora first seen at 20:45 and continued for half an hour with undiminished intensity. Aurora also seen low in north around 22:00.	Prescott Journal-Miner (1921)	Local time taken to be usual practice for most of Arizona, namely GMT - 7 hr. A newspaper search shows no evdience for use of DST in Prescott after 1919.
United States	15 May 1921 05:30	15 May 1921 07:45	Bright aurora observed from ship midway on trip from Puget Sound to Honolulu (33.18° N, 146.44° W). Bright rays seen from 20:30 to 21:15 local time, with bright red aurora to 21:30, then fading to nothing by 22:45	Lyman (1921)	Observations reported in local time. Take this as GMT-9h so start of observations matches end of NT at 05:30.
United States	15 May 1921 05:40	15 May 1921 07:15	Brilliant aurora seen from Lick Observatory on Mount Hamilton in California	Campbell (1921)	NT ended 04:10. Observations reported in Pacific time (GMT-8 hr)
Samoa	15 May 1921 05:45	15 May 1921 06:30	Red aurora observed up to 22 deg elevation in southern sky as seen	Angenheister and Westland (1921a)	NT ended 05:55. Observations reported in GMT

10.1029/2019SW002195

Table 3
(continued)

Country	Start time (GMT)	End time (GMT)	Observations	Reference	Notes
			from Apia Observatory (18:15-19:00 local time). Most intense around 06:20 GMT with intense aurora moving east to west, yellow streamer seen at this time.		
United States	15 May 1921 07:00		Spectacular auroral display seen from Bear Valley, San Bernardino. Peaking at 23:00 local time	San Bernardino Daily Sun (1921)	NT ended 03:40. Local time is GMT-8 hr

Note. Times of observations are converted to GMT where needed, using adjustments given in Notes column of this table. See text note S2 for further background on twilight times. Abbreviation: GMT, Greenwich Mean Time.

Thus, there was very noteworthy activity on 13/14 May, with observations and impacts that would be typical of a significant geomagnetic storm with Dst around -200 nT. But this activity was modest compared with what was about to happen in the early hours of 15 May.

3.2. Very Intense Activity, 14-15 May

After around 22:15 on 14 May the level of geomagnetic activity increased dramatically giving perhaps the most intense magnetic storm of the twentieth century, one that must be discussed alongside the Carrington event as a concrete example of how severe space weather is a natural electromagnetic hazard.

As noted in Figure 2a, this event started with an SC being observed at many geomagnetic observatories. For example, Alibag in India reported a sharp increase of 230 nT at 22:15 GMT (Chinmayanandam, 1921). However, others simply reported the sudden onset of large geomagnetic variations, for example, Apia in Samoa reported the onset at 22:13 of a "sinusoidal variation" with period of 2 hr (Angenheister & Westland, 1921a). Plate II of that paper shows that this was a wave-like field depression lasting about 2 hr and reaching a depth of around -150 nT before returning to previous values. This depression is also seen in detailed observations from Honolulu, some 4,200 km north-east of Apia (Kappenman, 2006) and in hourly values from Kakioka, 7,500 km to the north-west of Apia (Kunitomi, 1921). A similar but inverse wave-like variation was seen at sites in Europe. For example, Potsdam observations showed a wave reaching a maximum of +350 nT (perhaps after an SC of around 100 nT) before returning to previous values (see Figure 34a of Chapman & Bartels, 1940). A similar positive variation, following an SC, and a return to previous values, was seen at Tortosa, as shown in Figure 2 of Cortie (1921a); at Greenwich, as shown in Plate 1 of Dyson (1924); and at Rude Skov, as shown in Figure 41 of Stenquist (1925).

This large wave-like variation was just a start to the intense activity. It was quickly followed by around 7 hr of very intense activity between 01:00 and 08:00 on 15 May. At many observatories, the magnetic field measurements went off scale due to the intensity of the geomagnetic variations (see Table 1). Fortunately, this was not the case at the Apia observatory on the Pacific islands of Samoa. This provided an excellent and complete observation of how the storm intensified over a period of 6 hr, and then decayed over some 18 hr (Angenheister & Westland, 1921a). In particular, Plate II associated with that paper shows the variation of all three magnetic field components throughout the storm. An overview of that signature is reproduced in Figure 2b along with a similar signature observed at Kakoika observatory in Japan (Kunitomi, 1921). Taken together they show that there was an intense depression of H starting around 02:00 on 15 May, reaching a depth of 900 nT at 05:30. Following that there was a marked recovery by 06:00, another depression around 07:00, and then a gradual recovery over many hours. This depression is an outstanding feature of the 1921 storm and is associated with some fascinating effects including the following:

1. widespread disruption of telegraph, and some telephone, systems around the world as shown in Table 2 and Figure 2a, showing that this intense geomagnetic activity had generated strong geoelectric fields that drove GICs into vulnerable infrastructures;

2. observations of brilliant aurora around the world at midlatitudes, and in some cases to unusually low latitudes, as shown by the examples given in Table 3 and Figure 2a, showing that strong auroral currents in the ionosphere extended to much lower latitudes than normal; and
3. reports of improved propagation of radio signals over long distances (beyond the line of sight) in several parts of the world, perhaps an indication of enhanced ionization in the D region, as discussed in section 4.3.

We will discuss each of these effects in detail in the following sections, showing how they all provide evidence that this was a period of very intense space weather that caused major disruption and damage to vulnerable systems. That evidence shows that this was truly dangerous storm, since it led to impacts that put lives at risk. It was a spectacular space weather event that should be considered, alongside the Carrington event, in the generation of scenarios that we use in assessing and mitigating future risks from severe space weather.

4. Review of Impacts Reported During the Very Intense Activity

4.1. Impacts From GICs

The storm drove Earth currents into the telegraph systems that were then the backbone of telecommunications across the world and, in some cases, to the growing network of telephone lines. The list of impacts in Table 2 shows that these impacts were global with reports of disruption from Australia, Brazil, Denmark, France, Japan, New Zealand, Norway, Sweden, the United Kingdom, and United States. Many of these impact reports include useful timing information and show that the worst problems arose during those 7 hr of very intense activity between 01:00 and 08:00 on 15 May. These reports also show that telegraph operators had a good awareness of earth currents (as GIC was then known) with many operators reporting measurements of the strength of those currents and of the associated voltages. A good example of this awareness comes from New Zealand where operators were able to mitigate GIC impacts by switching from use of earth return (i.e., current return through the conducting Earth) to return via wires.

The most spectacular (and most dangerous) examples of GIC impact were two destructive fires—the first in Sweden around 02:00 GMT on 15 May and the second in the United States around an hour later (times shown in Figure 2a by the upper pair of magenta arrows) The Swedish event occurred in a telephone exchange in the town of Karlstad, 260 km west of Stockholm. This event was widely reported around the world (e.g., Fouche et al., 1921; New York Times (NYT), 1921c; Daily Herald, 1921; Belfast Telegraph, 1921; Sunderland Daily Echo, 1921). It was also the subject of contemporary study by David Stenquist, a Swedish scientist and engineer, who had a long interest in what we would now call GIC impacts on telecommunications systems. One of his narrative reports on the event is included in his 1925 memoir on earth currents (Stenquist, 1925), and another is reproduced by Karsberg et al. (1959). They both outline how the operators at Karlstad exchange first experienced problems (equipment anomalies and faint smoke) around 01:00, followed by a period of quiet, before the main fire started around 02:00 leading to extensive equipment damage. (The scale of that damage is recorded in contemporary photographs held by several Swedish museums, as discussed in the supporting information.) Stenquist also highlighted a near-miss incident at Ånge, some 380 km north west of Stockholm, that was simultaneous with the Karlstad fire. This experienced a threat similar to that fire, but where the initial problems were sufficient to trigger preventive measures that avoided major damage. In his later analysis of the Karlstad fire (Albinson, 2018; Engström, 1928; Stenquist, 1925), Stenquist noted that this site was vulnerable to strong GIC, because it was on the 400 km route of the major communications lines between Oslo and Stockholm, and this route was vulnerable because of its east-west orientation. His insights into engineering design of the communications lines enabled him to estimate the geoelectric fields that created the damaging GIC. He showed that fields of at least 6 V/km were required to cause the observed melting of fuses, "tubes de fusion," in copper wires, and that a field of 20 V/km would have caused more damage than observed (melting of fuses in iron wires). As a result he suggested that 10 V/km would be a reasonable estimate of the average geoelectric field in central Sweden at the time of the Karlstad fire. A later review of GIC impacts on wired telecommunications (Sanders, 1961) noted that in the case of the Karlstad fire, these fields would have been applied over a typical line length of 100 to 200 km, and thus concluded that the induced voltages on the lines into Karlstad would be of order 1,000 V.

The U.S. fire occurred in the village of Brewster in New York state, some 80 km north of New York city, between 03:00 and 04:00 GMT. The fire started in a switch-board at the Brewster station of the Central New England Railroad and quickly spread to destroy the whole building (Brewster Standard, 1921a; NYT, 1921c). The first reference notes that the night operator had to evacuate the building, rousing another person asleep in the building as well as saving some valuables. There is also evidence of significant damage elsewhere in the Northeast United States caused by GIC during this storm with communications being delayed on 16 May due to the need to repair damage such as burned-out equipment (Berkshire Eagle, 1921). One major example is that the Boston and Albany Railroad experienced damage to telegraph and telephone equipment in many places along its 250-km route between Boston and Albany (Springfield Republican, 1921). This reference notes that the damage was most significant in the western half of the route, which passed around 100 km north of Brewster. Unfortunately, the reference does not provide any detailed information on the times when damage occurred on the Boston and Albany systems. However, it does note that other railroads in the Northeast United States (e.g., New Haven, Boston and Maine) were much less affected and attributes the vulnerability of the Boston and Albany route to its east-west orientation. In contrast to Stenquist's analysis of the Karlstad fire, we do not appear to have any contemporary estimates of the geoelectric fields in the Northeast United States. However, there are many reports that induced voltages up to 1,000 V were measured on telegraph systems in that region (Lyman, 1921; NYT, 1921c; Telegraph and Telephone Age, 1921c). Such large voltages on telegraph lines are suggestive of geoelectric fields of order 10 V/km, as noted by Sanders (1961) in his discussion of the Karlstad fire. They are also consistent with Sanders' report that geoelectric fields of similar strength had been observed in the United States during earlier geomagnetic storms.

There is evidence that the large geoelectric fields in the Northeast United States also extended over the border into Canada. The Ottawa Journal (2006) reported that many long-distance telephone lines in New Brunswick were burned out by the storm, especially areas close to the U.S. border, some 700 km north east of Brewster. No specific times are available in that report but are available from measurements of GIC levels on an east-west telegraph line linking Montreal to Port Arthur, which is now part of Thunder Bay (Telegraph and Telephone Age, 1921a). These measurements were made at Capreol, Ontario, a telegraph station near the midpoint of this 1,200-km-long line and some 830 km north-west of Brewster. Measurements between 02:15 and 03:30 GMT (Telegraph and Telephone Age, 1921a) showed GIC levels up to 0.2 amps. Simple application of Ohm's law shows that this GIC level requires geoelectric fields up to 0.5 V/km (given a resistance of 2.6 ohm/km, as appropriate for the 9 gauge copper wire formed the line). A surge of much higher currents was observed at 03:30 GMT, causing heating and electrical discharges, such that all measurements were terminated so as to protect equipment. The dramatic nature of this surge suggests at least an order of magnitude increase in the geoelectric fields, occurring at more or less the same time as the Brewster fire above. Thus, it is reasonable to conclude that the intense geomagnetic activity led to strong geoelectric fields, up to ~10 V/km in the Northeast United States and adjacent regions of Canada, between 03:00 and 04:00 GMT.

Further afield, there were reports of damaging activity ("breaks and sparks") on Norwegian telegraph systems (Fouche et al., 1921), which is not surprising given the events that occurred in adjacent Sweden. What is perhaps surprising is the lack of reports of damage from other countries in Northern Europe. Reports from the United Kingdom (e.g., Chree, 1921b) show that there was significant disruption of telegraph traffic across Britain and Ireland but give no indication of damaging impacts. However, some UK newspaper reports (Belfast Telegraph, 1921; Sunderland Daily Echo, 1921) note that there were major impacts in Canada and Eastern Europe but give no further details.

The damage caused by this event also spread to the transatlantic cables then used to transmit telegraph messages between Europe and North America. A report in the New York Times (NYT, 1921c) gives some technical insight into the problem, suggesting that GIC in cable led to a breakdown of insulation at a weak point. The weak point could be located by resistance measurements from shore stations, so that a ship would be sent out to lift and repair the damaged section. While we lack specific timing of the cable fault within the storm, it is entirely reasonable to assume that it must have occurred during the intense geomagnetic activity between 01:00 and 08:00 GMT, and thus when we know that there were strong geoelectric fields that could have driven GIC through the cables. This is consistent with measurements made on cables during later major storms; for example, Sanders' (1961) review of GIC impacts on wireline communications describes similar disruption of cables during the major storm of 11 February 1958, a storm that also caused damage in Sweden comparable to the May 1921 events described above (Karsberg et al., 1959).

In summary, the intense geomagnetic activity between 01:00 and 08:00 on 15 May 1921 had a global impact on telegraph and telephone systems that were then key telecommunication technologies. The GIC was sufficiently intense to cause widespread damage, including at least two catastrophic fires, in the Northeast United States and Scandinavia; it also damaged transatlantic telegraph cables.

4.2. Extent of Auroral Observations

The aurora was widely seen around the world during this period, and some key examples are shown in Table 3 and Figure 2a. Many of these reports come from professional astronomers and official weather observers, which gives them a high degree of credibility, not least when their professionalism provides detail that can help us assess the evolution of the intense activity. Another valuable feature in these reports is a spread of observations across Europe and the United States, together with the short hours of darkness in these countries in May. The European observations sampled the early phase of the intense activity up to around 03:00 GMT, while the observations across the United States sampled later phases, as shown in Figure 2a.

A prime example in the European observations was those made by Bernard Lyot at Meudon. His observations are reported in Fouche et al. (1921) and show that he had prepared to observe through the night, after noting the strong geomagnetic activity that occurred during daytime hours of 14 May. His observations showed that there were peaks of auroral intensity at 01:14, 02:10, and 03:05, after which the light of dawn prevented further observations. The first peak was also recorded as a magnificent appearance ("prachtvolle Erscheinung") by astronomers in Breslau (now Wrocław), some 1,100 km east of Meudon, when seen around 01:30 just before the start of nautical twilight (Wilkens & Emde, 1921). Lyot noted that the peak at 02:10 was the most intense, a point confirmed by another French observer viewing the aurora from near Le Havre (Fouche et al., 1921), and by British observers near London and in East Anglia (Burns, 1921).

Moving across the Atlantic, the aurora was observed by a number of official observers working for the then U.S. Weather Bureau (now National Weather Service). A prime example was a report from an observer in Nebraska, who recorded a spectacular aurora, most intense between 03:30 and 04:30, soon after local dusk (Lyman, 1921). This aurora was also observed from other U.S. locations including San Antonio in Texas (Lyman, 1921), and Tucson and Flagstaff in Arizona (Douglass, 1921; Russell et al., 1921), and may well include an auroral arc ("the effect was like a curtain flapping in the wind") seen over New York (NYT, 1921a).

The observations from Tucson (Douglass, 1921) and Flagstaff (Russell et al., 1921) indicate that the aurora became less intense for a while around 05:30, but then showed a period of renewed activity. Some of this later aurora was also observed from a ship midway on a voyage from Puget Sound to Honolulu. The ship's captain reported seeing bright rays seen from 05:30 to 06:15, soon after local dusk, with later activity fading to nothing by 07:45 (Lyman, 1921). This aurora was simultaneous with the observation of aurora from Apia in Samoa in the equatorial Pacific region. The scientists operating the geophysical observatory at Apia reported seeing red aurora up to 22° elevation in the southern sky between 05:45 and 06:30, most intense around 06:20 (Angenheister & Westland, 1921a). Their report also notes that the aurora was seen at Tongatabu, the main island of Tonga, 900 km south-west of Apia. As noted by Silverman and Cliver (2001) and Cliver and Dietrich (2013), these observations are curious given the low magnetic latitude of Apia, but very credible given the professional background of the observers at Apia.

In summary, spectacular auroral displays occurred throughout the period of intense geomagnetic activity between 01:00 and 08:00 on 15 May 1921. As short night hours swept across Europe and North America, a host of observers sampled at least five peaks of major auroral intensity around 01:00, 02:00, 03:00, 04:00, and 06:00 GMT respectively. The auroral observations from Arizona (Douglass, 1921; Russell et al., 1921) confirm the reality of the longer gap between the last pair of peaks.

4.3. Impacts on Radio Propagation

Another interesting feature of this storm is a very variable impact on the propagation of long distance radio signals. There are reports showing both disruption and enhancement of radio propagation, with reports of enhancement gaining much attention because they were in stark contrast to the disruption of other telecommunications systems as discussed above (NYT, 1921d).

One example of enhancement was a report in the New York Times (NYT, 1921a) that radio signals reaching New York from Berlin (some 6,400 km distant) and Bordeaux (5,800 km) were much stronger than usual between 02:30 and 04:00 GMT on 15 May. This report has particular credibility because the New York Times was one of a number of U.S. newspapers that then operated their own radio stations to receive news from Europe (Hudson et al., 2000). The good performance of radio links in the United States and at Bordeaux was also confirmed in statements by the Radio Corporation of America (Telegraph and Telephone Age, 1921b). Another example of enhancement came from the Pacific region, where Angenheister and Westland (1921a) and Gibbs (1921) reported unusually good conditions around 06:15 on radio links between radio stations at Apia in Samoa and Awanui in the north of New Zealand (a distance of 2,700 km). The times of these two enhancements are shown by the lower pair of magenta arrows in Figure 2a.

However, Gibbs (1921) also reported that there were problems during 15 May (also 14 and 16 May) with radio links within New Zealand, and between New Zealand and Australia; signals were “erratic in intensity and uniformity.” He also noted that the great variations in these radio signals were simultaneously accompanied by earth currents in telegraph lines serving New Zealand's network of radio stations. Problems with radio links were also reported from the United States. Lyman (1921) includes a report that the radio station at Fort Sam Houston near San Antonio was rendered useless at times due to heavy static accompanying the aurora. A report in Omaha Daily Bee (1921) noted that use of radio by the local air mail station was shut down, whilst a report in the Great Falls Tribune (1921) noted considerable interference with maritime use of radio all along the west coast of North America and in the Philippines.

To understand the enhancement of radio signals during the storm, it is essential to appreciate that the radio systems in use in 1921 operated in low-frequency radio bands below 300 kHz. For example, the radio link between New Zealand and Samoa operated at 150 kHz (Gibbs, 1921). At this frequency, radio signals couple to the conductive surface of the Earth, both land and sea, and propagate along that surface, following the curvature of the Earth in a so-called “ground wave.” The signals are gradually attenuated by the finite conductivity of the surface with less attenuation where conductivity is higher, mostly obviously over the salt water that forms the oceans (International Telecommunications Union, 2007). However, the signals can also propagate into the upper atmosphere and be reflected from the ionosphere giving a “sky wave” that can interfere with the ground wave signal, causing problems with signal reception. Sky wave interference can also arise from distant sources of natural radio signals such as lightning and other electrical activity in the atmosphere. Thus, good conditions for signal propagation at 150 kHz will arise when sky waves are heavily attenuated by absorption due to significant plasma density in the lower ionosphere below 90 km (*D* region). This is the case during daytime hours as solar ultraviolet radiation from the Lyman-alpha emission line penetrates to these attitudes. Indeed, Gibbs (1921) notes that it was well known from practical experience that propagation was better in daytime. However, the enhanced propagation between Apia and Awanui occurred about an hour after sunset at both sites. This suggests that the storm had enhanced the *D* region along the path between these sites. Given that this effect was simultaneous with the observation of aurora in this region (Angenheister & Westland, 1921a; Silverman & Cliver, 2001), it suggests that the keV electron precipitation that generated the visible aurora was accompanied by higher energy electrons that could penetrate below 90 km and generate *D*-region ionization.

Turning to the transmissions from Berlin and Bordeaux to New York discussed above, these used the German government's Nauen transmitter, which operated on lower frequencies, between 17 and 50 kHz (Huurdeman, 2003), and the Franco-American transmitter at Bordeaux-Lafayette which operated at 15 kHz (Dessapt, 2012). At these frequencies, radio signals can propagate very long distances (thousands of kilometers) as sky wave reinforces the ground wave such that the region between the ground and the ionosphere acts a natural waveguide (Barclay et al., 2002). This mode enabled early radio systems to work over the oceans, as on the transatlantic routes where signal strengths were enhanced at the same time as bright aurorae were observed both in France and the United States, as discussed above. This suggests that electron precipitation associated with the aurora may have enhanced transatlantic propagation, perhaps creating a steep vertical gradient in plasma density at base of the ionosphere, such that the very low frequency radio waves used by the Nauen and Bordeaux-Lafayette transmitters were strongly reflected, rather than absorbed.

In summary, the May 1921 storm caused a mixture of disruption and enhancement to radio communications. There are two well-reported enhancement events, one over the Atlantic and one over the Pacific, both simultaneous with the observation of aurora close to the path of the radio signals. It is plausible that relativistic electron precipitation, simultaneous with the lower energy electrons that produce the aurora, generated additional ionization in the lower ionosphere. This could have aided radio propagation by modifying sky wave propagation both by increasing skywave reflection at VLF frequencies (as on transatlantic routes) and by increasing skywave absorption at higher frequencies (as between New Zealand and Samoa).

5. After Effects

5.1. Geomagnetic and Auroral Observations

The intense activity between 01:00 and 08:00 GMT on 15 May was not the end of storm. Lesser activity continued through the rest of 15 May, quieter after around 12:00 as noted by Lemos (1921) in measurements from Brazil and as shown in the Christchurch and Greenwich measurements presented, respectively, in Plate I of Skey (1921) and Plates II and III of Dyson (1924). An isolated substorm occurred around 10:30 to 11:00 as shown by a marked depression in H (>600 nT) in Sitka magnetometer data (Kappenman, 2006), and a smaller depression (~200 nT) in the H trace from Christchurch (Skey, 1921).

There was also renewed activity on 16 May following another SC at 01:24 that day (Observatori de l'Ebre, 2019) as shown in Figure 2a. This SC was seen at Apia (Angenheister & Westland, 1921a) with amplitude around 50 nT, followed by a depression in H, typical of enhanced ring current, starting around 03:30, with distinct minima around 07:00, 10:00, and 12:00 with depths of 200, 240, and 200 nT, respectively. Measurements at other locations confirm that this was a period of significant magnetic activity. Skey (1921) noted that measurements at Christchurch in New Zealand showed "a recrudescence of effects" seen previously, but that these later effects were "milder." Parkinson (1921) noted magnetic disturbances at Watheroo between 08:00 and 16:00; together with personal observations of aurora from that same location between 11:55 and 12:07. Chinmayanandam (1921), working at Alibag, noted that another depression in H started around 04:40 and that H went off scale around 09:15. The Greenwich measurements (Dyson, 1924) show a similar effect with N off scale between 08:20 and 09:10 indicating a depression in N that was >450 nT. This large depression was also observed at Tortosa in Spain, with H off scale between 08:00 and 10:00 (Rodes, 1921). Significant activity in this period was also noted in Brazil (Lemos, 1921) and the United States (Hartnell, 1921).

In summary, there was major geomagnetic activity in the hours and days following the intense geomagnetic activity that is the heart of the May 1921 storm. This suggests that the Sun continued to produce strong CMEs as a result of activity driven by magnetic complexity that was observed in Mount Wilson region 1842 (Lundstedt et al., 2015). This latter solar and geomagnetic activity is not directly relevant to the main focus of this paper, namely, the intense activity on 15 May, but is included here to provide a more complete picture of the May 1921 storm. That complete picture is important for future work to develop exercise scenarios based on this storm and to provide context for the New York fire that we will now discuss.

5.2. The New York Railroad Fire

At 11:04 GMT on 15 May a major fault disrupted electrical systems controlling train movements along 6 km of the major rail line that runs northeastward out of New York's Grand Central station (NYT, 1921b). This was followed by a serious fire that destroyed a control tower located about 1 km from Grand Central. Trains in and out of Grand Central were significantly delayed as the staff used manual procedures to allow safe movement of trains, while the electrical systems were repaired. The disruption was reported in newspapers on 16 May (as in the NYT article cited above) and, perhaps unsurprisingly, was associated by them with the intense geomagnetic activity in the early (GMT) hours of 15 May, activity that had been widely reported in the previous day's newspapers.

However, this association is weak when we look at details. As shown by the magenta arrow marked "NYC fire" in Figure 2a, the disruption occurred several hours after the end of the intense geomagnetic activity. Thus, it seems unlikely that earth currents could have disrupted rail control systems at 11:04. There was some modest geomagnetic activity in the hour prior to the disruption, as noted above, but this seems to have its largest impacts in the Pacific region, for example, at Sitka in Alaska and Christchurch in New Zealand.

There is no evidence for strong activity in the region around New York. The report of geomagnetic activity observed at Cheltenham, Maryland, 330 km south-west of New York, explicitly notes that there was "a period of comparative quiet" between 09:00 and 22:00 on 15 May (Hartnell, 1921).

The weakness of the association is reinforced by later newspaper reports. On 17 May, the New York Times reported remarks by the head of the electrical division of the New York Central railroad (NYT, 1921c). He noted that there had been a short circuit when a breakdown of insulation had allowed the power supply to electric trains ("third-rail" technology still widely used today, e.g., on metro systems) to come into contact with a water pipe. He considered that this could explain the disruption and fire without the need to invoke earth currents (though he did also note candidly that he wished he could prove earth currents were involved "because it would make a good alibi for me").

Given the timing of the rail disruption away from intense geomagnetic activity, and the identification of a simple engineering fault as a plausible cause of the disruption, we can firmly reject the association of the New York railroad fire with space weather. This much-cited example of space weather impacts needs to be reconsidered. While it does not stand up as a direct example of space weather impact, it is an excellent example of how apparent association can gain traction through publicity in the media. It shows the importance of putting reported impacts in context of our scientific understanding of space weather.

6. Discussion

The great geomagnetic storm of May 1921 took the classic form of such events in that it was linked to passage of a major active region across the central meridian of the Sun as seen from Earth. Detailed solar observations from Mount Wilson in California show the region was magnetically complex and productive of solar flares (Lundstedt et al., 2015). Magnetometer measurements across the Earth show that there were a series of SCs during this period, strongly suggesting that the Earth was bombarded by a series of coronal mass ejections linked to this region.

The storm produced three major periods of geomagnetic activity as shown by the strong red bars in Figure 2 a. There was also additional lesser activity at other times, particularly at high latitudes. In most circumstances, the first and third periods would have been regarded as major events in their own right, matching and probably outranking any of the events observed during recent solar cycle 24. But in this case they were dwarfed by the intense activity, and the damaging and disruptive impacts, generated by the second event, which is a key focus of this paper.

The first period of activity may also have played a significant role in preparing the way for the main event on 14/15 May. The CMEs that generated strong activity on 13/14 May may have swept plasma out of the inner heliosphere so that a later CME could travel more quickly to Earth, as previously suggested by Lundstedt et al. (2015). Thus, it was able to deliver a large amount of energy into a magnetosphere that was already active, leading to very intense space weather on our planet—as we shall now discuss.

That intense space weather at Earth began with a sharp onset of strong global geomagnetic activity soon after 22:00 GMT on 14 May as noted in most of the observatory reports summarized in Table 1. We lack insights into the specific solar activity that led to this onset. However, given our modern understanding of the underlying science, a large fast CME probably left the Sun early on 14 May, leading to the arrival of the CME shock soon after 22:00, as indicated by the SC observed at several magnetometer stations. A reasonable transit time for this CME is between 12 and 18 hr, that is, in the range between the known transit times of the CMEs that drove the great storms of 1972 and 1859, respectively (Cliver & Svalgaard, 2004). Thus, it would be interesting to look for signatures of a CME launch, particularly between 04:00 and 10:00 on 14 May. Such a search is beyond the scope of this paper, but it is worth noting that many magnetic observatories were on the dayside in that period and thus were well-placed to see the magnetic crochet that would have occurred if a large flare was associated with the CME launch.

Following that sharp onset, there was first a slow global oscillation, lasting around 90 min, manifesting as a dip in H at low-latitude sites such as Apia, Honolulu, and Kakioka, and as a peak at midlatitudes sites in both hemispheres, for example, Christchurch, Greenwich, and Potsdam. This was followed by an hour of shorter period variations before the onset of the most intense activity. The very intensity of this later activity makes it hard to extract a pattern from geomagnetic reports, other than the gradually increasing depression of H at low-latitude stations as shown in Figure 2b. In contrast, the auroral and impact reports from this later activity do show a pattern. The auroral reports show that there was a series of displays of bright aurora with peaks around 01:00, 02:00, 03:00, 04:00, and 06:00, suggesting that a series of five intense substorms created those displays (Akasofu, 1964). Some of the auroral peaks were also associated with impacts on telephone and telegraph systems, as we would expect if those substorms generated strong geoelectric fields A similar association of substorms with geoelectric field impacts on power systems in Canada and the UK during the March 1989 storm was noted by Eastwood et al. (2018)—see their Figure 1a. The reduced activity between 04:00 and 06:00 is also confirmed by a report of a brief respite in telegraph disruption in Phoenix, Arizona (Arizona Republican, 1921a). This respite around 05:30 matches reports of reduced auroral activity as seen from observatories in other parts of Arizona (Douglass, 1921; Russell et al., 1921).

Looking in more detail at the possible substorm timeline and its impacts, the first three correspond to the peaks of auroral intensity seen by Bernard Lyot at Meudon (Fouche et al., 1921), with the fourth and fifth after dawn at Meudon but well observed in the United States and eastern Pacific (Douglass, 1921; Lyman, 1921; Russell et al., 1921). The first two substorms match the times, respectively, of the initial problems at Karlstad and Ånge, and then the catastrophic fire at Karlstad, all as described in Stenquist (1925) and Karsberg et al. (1959). The third and fourth substorms match the time of the catastrophic fire at Brewster (Brewster Standard, 1921a) and the GIC surge at Capreol (Telegraph and Telephone Age, 1921a), as well as the enhanced very low frequency radio propagation across the Atlantic (NYT, 1921a), which we have attributed to high-energy electron precipitation alongside precipitation of keV electrons that generate aurora. This rapid sequence of substorms also provides a good explanation for the gradually increasing depression of H at low latitudes—in that such repeated substorms could inject particles into the ring current, building up its intensity to produce a large depression of H by 05:30, as shown in Figure 2b.

The fifth substorm matches both the enhanced radio propagation at 150 kHz that was reported on the link between Apia and New Zealand (Gibbs, 1921), and the observation of aurora from Apia (Angenheister & Westland, 1921a). This final substorm also matches the rapid 400 nT recovery of H in the Apia magnetic data, as shown in Figure 2b. This abrupt rise in H is curious in that it is much too fast to be the result of normal ring current decay. Cliver and Dietrich (2013) have noted that such rapid changes are more typically of fluctuations in the auroral electrojet and thus suggest that the aurora seen from Apia was associated with an eastward electrojet. An eastward current system would be expected at that local time (early evening) and could explain the rapid rise and fall of the Apia H component around 06:00. Note that, after 07:00, the Apia H component rises again, but more slowly as we would expect from normal ring current decay.

This sequence of intense substorms suggests that the interplanetary magnetic field (IMF) turned strongly southward soon after 00:00 GMT on 15 May and remained strongly southward for the duration of these events, except for the longer gap between 04:00 and 06:00. The substorm timing, starting 2 hr after arrival of the CME shock, suggests that the southward IMF was the magnetic field in the leading part of a flux rope that formed the CME. This configuration, as part of a fast CME, would have driven a large flow of solar wind energy into the magnetosphere, the flow required to drive repeated Dungey cycles in the magnetosphere, and hence the intense geomagnetic and auroral activity that was observed around the world. The short quiet period around 05:30—as noted in the auroral observations by Douglass (1921)—followed by the fifth substorm may indicate that a second CME had caught up with the first, compressing northward IMF in the tail of the first CME, and perhaps with additional southward IMF in the leading part of the second CME. Such a CME-CME interaction could also have helped to sustain CME speed and hence added to the geoeffectiveness of these CMEs (Liu et al., 2014; Lugaz et al., 2017).

The final period of activity on 16 May started with another SC at 01:24, suggesting the arrival at Earth of another major CME. The ensuing activity may be summarized as a moderate storm with a modest enhancement of the ring current, significant geomagnetic activity at midlatitudes and aurora observed at dark sites at midlatitudes. This third period was much milder than the second period, but it does demonstrate how there can be significant space weather conditions in the days following a severe event.

In summary, the May 1921 storm exhibited a series of features that can inform our understanding of severe space weather and help us plan for future severe events. The storm was undoubtedly driven by the arrival at Earth of a series of major coronal mass ejections, as indicated by the series of SCs (Observatori de l'Ebre, 2019). There were three periods of major geomagnetic activity, all producing significant geomagnetic effects and impacts at midlatitudes, and, in the case of the first and second periods, some outstanding features that are worth highlighting.

The first period included a large spike-like depression of the horizontal geomagnetic field in the region around Copenhagen, and that produced significant disruption of telephone services between that city and major cities in Sweden. This spike event may be similar to those recently identified by Cid et al. (2015) and Saiz et al. (2016), events that could induce large geoelectric fields, and that are now an important research target. Thus, the 1921 spike event is an excellent addition to the scenario that is the main goal of this paper, as well as evidence that may be useful for wider studies of spike events.

The second period caused damage, in the form of fires, which posed a significant risk to life. Thus, this second period was truly dangerous and is the driver for the title of this paper. It included a number of extreme physical effects including the following:

1. Geoelectric fields around 10 V/km were found to have occurred in Sweden, leading to disruption and damage to Swedish telecommunications networks, most particularly the major fire that destroyed the major communications center in Karlstad.
2. Similarly, intense geoelectric fields probably occurred in parts of the Northeast United States, and adjacent regions of Canada, leading to damage to communications networks, particularly those vital to railroad operations. The major fire that destroyed Brewster station is a notable example of this.
3. A huge depression of the equatorial magnetic field at Apia, suggesting an extremely large ring current. While this ring current is not a driver of the large geoelectric fields above, it is important in understanding the low-latitude geomagnetic observations.

The breadth and depth of evidence about the May 1921 storm suggest that it can provide an excellent basis for developing severe space weather scenarios. Such scenarios are now a vital tool in planning for future severe space weather, as discussed above. The 1921 storm includes a number of features that can make for a well-rounded scenario, including substantial precursor activity, a very severe main phase, and continuing activity after the main phase. The precursor activity provides an example of how the inner heliosphere and magnetosphere may be preconditioned such that a subsequent major CME is very geoeffective, leading to extreme geomagnetic fields in regions with resistive geologies. The later continuing activity demonstrates the challenge of knowing when the storm is over. An important scientific element in managing future space weather events will be to determine when we can declare "all clear," that we are confident the storm is over and recovery work can begin in earnest.

The 1921 storm also includes some examples of how other problems might confuse the "information picture" that will be used by emergency managers during a severe space weather event. A key example is the New York railroad fire discussed above. As we have shown above, it is unlikely this was caused by space weather, but it is understandable how an apparent link to space weather was perceived at the time. Another, more curious, example is a report in the New York Times (NYT, 1921f) that the disruption of telegraph services in France had "not been marked by any exceptional appearance of the aurora." As the reports by Fouche et al. (1921) make clear, there were many observations of spectacular aurora from France, not least from Paris. In this instance, the sources of the report clearly had an incomplete set of information, perhaps because the spectacular aurora occurred well after midnight local time. Both examples show the importance of scientific advice in assessing real space weather impacts, and distinguishing them from coincidence, factors that are recognized in governmental planning to manage natural hazards of all kinds. The contemporary importance of such advice is demonstrated by recent experience in Mexico in September 2017, when severe space weather coincided with the impact of a hurricane and a major earthquake. Scientific advice was important in helping civil protection authorities to address these different hazards and, most importantly, to counter scare-mongering that created unnecessary public anxiety about the coincidence of these hazards (Gonzalez-Esparza et al., 2018).

7. Conclusions

The great geomagnetic storm of May 1921 produced extreme geophysical conditions, in particular large geoelectric fields (~10 V/km) in several parts of the world. Such large fields are a major concern today because of their potential to impact contemporary technologies such the transmission of electrical power (Pulkkinen et al., 2017), railway track circuits (Krausmann et al., 2015), and cathodic protection systems for pipelines (Gummow, 2002). The May 1921 storm therefore provides a well-documented historical example that can inform future decisions on the risk that space weather poses to such systems, taking account of how regional differences in the value and complexity of ground conductivity may decrease or increase the risk. It is an important element in the assessment of worst-case scenarios for severe space weather conditions (Hapgood et al., 2016; National Science and Technology Council, 2018).

However, as discussed above, the scientific development of space weather scenarios must go well beyond the parameterization of worst-case environments. We need to provide timelines showing how those environments may wax and wane during a severe space weather event, outlining how events may develop, and how they may exhibit a mixture of minor and major peaks. Such timelines are an essential tool for policy-makers developing and testing societal resilience to space weather. It is important to have a variety of scenarios, so that policy-makers can explore different possibilities and be ready to respond flexibly to however a future space weather event manifests at Earth. The 1921 space weather event is therefore a valuable addition to existing scenarios based on the events of 1859, 1989, and 2003. In particular, it provides an outstanding example in the short but very intense geomagnetic activity that occurred between 01:00 and 08:00 on 15 May 1921.

Space weather scenarios can also provide a valuable challenge to scientific modeling of space weather, in particular of the magnetosphere-ionosphere-thermosphere system. The 1921 event includes several curious features that warrant investigation by modelers, for example, the large oscillation in the geomagnetic field seen just before the very intense activity early on 15 May, and also the rapid and fall in H seen at Apia, around 06:00 on 15 May. Could this latter feature be the result of the auroral electrojet reaching low latitudes as suggested by Cliver and Dietrich (2013)?

Finally, it is worth noting that we can probably do more to flesh out what happened in 1921. One obvious approach would be digitization of the magnetometer measurements outlined in section 3, where the photographic records of those measurements still exist in good condition. A first step would be digitization of the images of those records, for example, as has been done in the United Kingdom (see https://www.bgs.ac.uk/data/Magnetograms/home.html), and more recently in Russia (Ptitsyna et al., 2018). But the more difficult step is to gather the expertise and resources to extract numerical data from those records. Another important approach is to search for more evidence of solar flares during this period, most obviously searching geomagnetic records for the sharp pulses, magnetic crochets, that are clear signatures of X-class flares (for example, see Curto et al. (2018) for a discussion of the crochets produced by the X9 flare that occurred on 6 September 2017). Such large flares are frequently associated with the launch of major CMEs: a good example being the crochet observed by the Kew magnetometer just prior to the 1859 storm (Stewart, 1861). The lack of reports of crochets in accounts of magnetometer observations from May 1921 is curious, to say the least, and needs to be investigated more deeply. Is it just that we have not looked deeply enough into the data? Given the global network of magnetometers that existed in 1921 and the favorable timing of the event for observations from the Northern Hemisphere (i.e., long hours of daylight in May), a real absence of crochets would imply that this series of major geoeffective CMEs occurred without large flares. That would be a challenging result, so further investigation is needed.

A deeper analysis of magnetometer records could also enable a better assessment of the minimum Dst value for the May 1921 storms. Kappenman (2006) has suggested that the deep depression of H measured at Apia, as shown in Figure 2b, indicates a minimum Dst around -900 nT, much lower than the lowest value in the modern observational record (-589 nT during the March 1989 storm). Detailed analysis of low-latitude magnetometer data from sites at several other longitudes (compared to Apia) could help to confirm Kappenman's suggestion.

Another challenging issue is to determine whether there was a ground level enhancement (of cosmic radiation) during this event, indicating a large solar radiation storm with significant fluxes at GeV energies. There was no routine monitoring of radiation in 1921, but can we find any proxies through impacts on technologies then in-use or through the continuing improvements in studies of cosmogenic isotopes such as ^{10}Be? It would be valuable if space weather scenarios based on 1921 event could include radiation storms.

Acknowledgments
All data used in this paper is properly cited and sourced either from papers in the reference list or from publicly available tools described in the text. Access to these data has been greatly aided by the many scientific societies and publications that have kindly made their old journal issues readily available online. The list is too long to put here but can be seen from many old papers listed in the references. But I would like to explicitly thank SAO and NASA for the central role of their Astrophysics Data System in digitizing and openly disseminating many of these old papers. I also thank the Library at Rutherford Appleton Laboratory for their help in sourcing old papers not openly available online, notably some of those in Nature, and those in the New Zealand Journal of Science and Technology. More thanks go to the Radcliffe Science Library at the University of Oxford for the loan of their copy of Stenquist's 1925 memoir on his studies of Earth currents, also to the Bibliothèque nationale de France (http://www.bnf.fr/) whose digital library, Gallica, is an excellent resource for French newspapers and scientific journals from 1921, and to the Brandskyddsföreningen Sverige, which kindly supplied me a copy of the 1928 article by Engström. Images of the destruction at Karlstad telephone exchange have been put online by two museums: the collection of images from the former Svenska Telegrafverket, now held by the Tekniska Museet in Stockholm, is available on (https://www.flickr.com/photos/tekniskamuseet-telehistoriska/), while the collection of local images held by the Värmlands Museum in Karlstad is available on https://digitaltmuseum.org/owners/S-VLM. Further thanks are due to the Brewster Public Library, which has provided an archive of the Brewster Standard newspaper as part of NYS Historic Newspapers project (http://nyshistoricnewspapers.org/brewster/) and also to the Chronicling America project at the U.S. Library of Congress (https://chroniclingamerica.loc.gov/) for access to archives of several other newspapers including the Great Falls Tribune, Idaho Recorder, and Manning Times. I also thank the Connecticut Historical Society; volume 50 of their online archive of the Mary Morris Social Scrapbooks includes two pages of newspaper clippings devoted to the May 1921 storm; these provided me with clues on where to find more information about impacts of the storm on several railroads in the Northeast United States. See https://chs.org/finding_aides/mmsocial/V50-May1921-July1921p.pdf. Other newspaper

But the search for further evidence should not be limited to scientific data. Are there more engineering reports to be found, for example, similar to those of Gibbs (1921), Telegraph and Telephone Age (1921), and Stenquist (1925)? Or reports of work by skilled amateurs such as radio enthusiasts? The latter may have potential as high-frequency radio communications, where space weather has major impacts, was then the preserve of amateurs, many of them ex-military radio operators (Huurdeman, 2003). Finally another important source of information is further exploration of old newspaper reports. The increasing digitization of old newspapers will make such searchers tractable. Key areas for studies include Scandinavia, where we know impacts occurred, and hence, it would be good to expand our understanding. Eastern Europe is another important area where studies may be valuable since some UK newspaper reports of the impacts of the storm note that "the disturbing currents were particularly violent in Russia and Eastern Europe," but give no further details (Belfast Telegraph, 1921; Sunderland Daily Echo, 1921). It is important, though, to recognize that there was much political turbulence in Eastern Europe at that time, and thus, further work is needed to assess how that turbulence affected reporting of events such as the impact of the May 1921 space weather event.

References

Akasofu, S.-I. (1964). The development of the auroral substorm. *Planetary and Space Science*, *12*(4), 273–282. https://doi.org/10.1016/0032-0633(64)90151-5

Albinson, B, (2018) Artiklar från Värmlands Brandhistoriska Klubb. http://www.brandhistoriska.org/artiklar/artiklar.pdf (Last accessed 29 January 2019)

Allen, S (2019) Time scales, https://www.ucolick.org/~sla/leapsecs/timescales.html (Last accessed 27 April 2019)

Angenheister, G., & Westland, C. J. (1921a). The magnetic storm of May 13–14, 1921: Observations at Samoa Observatory. *New Zealand Journal of Science and Technology*, *4*, 201–202. NB Plate II of this paper is located between pages 200 and 201.

Angenheister, G., & Westland, C. J. (1921b). The magnetic storm of May 13–16, 1921, at Apia Observatory, Samoa. *Journal of Geophysical Research*, *26*(1, 2), 30–31. https://doi.org/10.1029/TE026i001p00030

Arizona Republican (1921a) Aurora borealis gives wonderful exhibition in northern skies, The Arizona Republican, 15 May 1921, Front page, top of rightmost columns

Atlanta Constitution (1921) Aurora borealis halts telegraph service to city, Atlanta Constitution May 15, 1921, front page.

Baker, D. N., Li, X., Pulkkinen, A., Ngwira, C. M., Mays, M. L., Galvin, A. B., & Simunac, K. D. C. (2013). A major solar eruptive event in July 2012: Defining extreme space weather scenarios. *Space Weather*, 585–591. https://doi.org/10.1002/swe.20097

Barclay, L., Hall, M. P. M., Craig, K. H., Bacon, D. F., & Hewitt, M. T. (2002). *Propagation of Radiowaves (Electromagnetics and Radar)*, (2nd ed.). London: section 18.4.2. Institution of Engineering and Technology. ISBN-13: 978-0852961025

Belfast Telegraph (1921) Storm in the Sun, Belfast Telegraph, 18 May 1921, page 7, 4th column, 2nd item.

Berkshire Eagle (1921) Aurora Borealis is still a little busy. The Berkshire Eagle. 16 May 1921, page 1, second column from left, 4th item.

Bleaney, B. I., & Bleaney, B. (1965). *Electricity and Magnetism*, (Vol. 2). Oxford University Press.

Brewster Standard (1921a) Aurora borealis burns depot, Brewster Standard, 20 May 1921, front page, rightmost column, first article.

Brooke, C., & Airy, G. B. (1847a). On the automatic registration of magnetometers, and other meteorological instruments, by photography. *Philosophical Transactions of the Royal Society of London*, *137*, 58–68. https://doi.org/10.1098/rstl.1847.0007

Brooke, C., & Airy, G. B. (1847b). On the automatic registration of magnetometers, and other meteorological instruments, by photography. *Philosophical Transactions of the Royal Society of London*, *137*, 69–77. https://doi.org/10.1098/rstl.1847.0008

Burns, G. J. (1921). Reports of the observing sections: Aurora and zodiacal light section. *Journal of the British Astronomical Association*, *31*, 329–330. ADS Bibliographic Code: 1921JBAA31329B

Cabinet Office (2015), Space weather preparedness strategy, Rep. BIS/15/457 UK Government, Department for Business Innovation and Skills London.

Campbell, W. W. (1921). The aurora borealis of May 14, 1921. *Publications of the Astronomical Society of the Pacific*, *33*(193), 164–167. https://doi.org/10.1086/123063

Cannon, P., Angling, M., Barclay, L., Curry, C., Dyer, C., Edwards, R., et al. (2013). *Extreme space weather: impacts on engineered systems and infrastructure*. London: UK Royal Academy of Engineering. 1-903496-95-0

Chapman, S., & Bartels, J. (1940). *Geomagnetism*. Oxford: Clarendon Press.

Chinmayanandam, T. K. (1921). The magnetic storm of May 13–17, 1921, at Alibag Observatory, India. *Journal of Geophysical Research*, *26*(1, 2), 28–29. https://doi.org/10.1029/TE026i001p00028

Chree, C. (1921a). The magnetic storm of May 13–17. *Nature*, *107*(2690), 359. https://doi.org/10.1038/107359a0

Chree, C. (1921b). The Recent magnetic and electrical disturbances. *Nature*, *107*(2691), 399. https://doi.org/10.1038/107399a0

Cid, C., Saiz, E., Guerrero, A., Palacios, J., & Cerrato, Y. (2015). A Carrington-like geomagnetic storm observed in the 21st century. *Journal of Space Weather and Space Climate*, *5*, A16. https://doi.org/10.1051/swsc/2015017

Cliver, E. W., & Dietrich, W. F. (2013). The 1859 space weather event revisited: Limits of extreme activity. *Journal of Space Weather and Space Climate*, *3*, A31. https://doi.org/10.1051/swsc/2013053

Cliver, E. W., & Svalgaard, L. (2004). The 1859 solar–terrestrial disturbance and the current limits of extreme space weather activity. *Solar physics*, *224*(1-2), 407–422. https://doi.org/10.1007/s11207-005-4980-z

Columbia Evening Missourian (1921). Sky show plays havoc, The Columbia Evening Missourian, 16 May 1921, Front page, second article in second column from left.

Cortie, A. L. (1921a). The sun-spot group and the magnetic disturbances, 1921 May 8-21. *Monthly Notices of the Royal Astronomical Society*, *81*(8), 515–520. https://doi.org/10.1093/mnras/81.8.515

Cortie, A. L. (1921b). The Great Sun-spot Group and Magnetic Disturbances, May 8–21. *Nature*, *107*(2692), 426–427. https://doi.org/10.1038/107426a0

articles were sourced using commercial services including newspapers.com for Canadian and U.S. articles and the British Newspaper Archive for UK articles (https://www.britishnewspaper-archive.co.uk/). M. H. was partly supported by STFC in-house research award ST/M001083/1.

Curto, J. J., Marsal, S., Blanch, E., & Altadill, D. (2018). Analysis of the solar flare effects of 6 September 2017 in the ionosphere and in the Earth's magnetic field using spherical elementary current systems. *Space Weather*, *16*, 1709–1720. https://doi.org/10.1029/2018SW001927

Dessapt, P. (2012) La Station Radio de Bordeaux-Lafayette. Raconte-moi la radio web site. http://leradiofil.com/lafayette.htm (Last accessed 13 January 2019).

Douglass, A. E. (1921). The aurora of May 14, 1921. *Science*, *54*(1383), 14–14. https://doi.org/10.1126/science.54.1383.14

Dyson, F. W. (1924). Results of the magnetical and meteorological observations made at the Royal Observatory, Greenwich, in the Year 1921. Greenwich Observations in Astronomy, Magnetism and Meteorology made at the Royal Observatory, Series 2, 83. ADS code: 1924GOAMM..83E...2D

Eastwood, J. P., Hapgood, M. A., Biffis, E., Benedetti, D., Bisi, M. M., Green, L., et al. (2018). Quantifying the economic value of space weather forecasting for power grids: An exploratory study. *Space Weather*, *16*, 2052–2067. https://doi.org/10.1029/2018SW002003

Engström, A. (1928) Jordströmmar såsom brandstiftare. Svenska Brandskyddsföreningens Tidskrift, Mai 1928. 77-79.

Fouche, M., Lyot, B., Esclangon, E., & Stormer, C. (1921). La Perturbation Magnetique du 14 au 16 Mai, l'Aurore Boreale et les Taches du Soleil. *L'Astronomie*, *35*, 225–237.

Gibbs, A. (1921) Effects of the recent aurora on telegraph-lines, telephone-lines, and wireless stations. *New Zealand Journal of Science and Technology*, *4*,183–188.

Gonzalez-Esparza, J. A., Sergeeva, M. A., Corona-Romero, P., Mejia-Ambriz, J. C., Gonzalez, L. X., de la Luz, V., et al. (2018). Space weather events, hurricanes, and earthquakes in Mexico in September 2017. *Space Weather*, *16*, 2038–2051. https://doi.org/10.1029/2018SW001995

Great Falls Tribune (1921) Aurora 'Breaks' Alaska 'Wires', The Great Falls Tribune, 17 May 1921, Page 2, 5th column from left

Gummow, R. A. (2002). GIC effects on pipeline corrosion and corrosion control systems. *Journal of Atmospheric and Solar-Terrestrial Physics*, *64*(16), 1755–1764. https://doi.org/10.1016/S1364-6826(02)00125-6

Hapgood, M. A. (1992). Space physics coordinate transformations: A user guide. *Planetary and Space Science*, *40*(5), 711–717. https://doi.org/10.1016/0032-0633(92)90012-D

Hapgood, M. (1997). Corrigendum, space physics coordinate transformations: A user guide. *Planetary and Space Science*, *45*(8).

Hapgood, M. (2018). Space weather: What are policymakers seeking? In *Extreme Events in Geospace*, (pp. 657–682). Elsevier. https://doi.org/10.1016/B978-0-12-812700-1.00027-3

Hapgood, M., Angling, M., Attrill, G., Burnett, C., Cannon, P., Gibbs, M., et al. (2016). Summary of space weather worst-case environments. Revised edition. RAL Technical Report RAL-TR-2016-06. http://purl.org/net/epubs/work/25015281. Last accessed 1 February 2019.

Hartford Herald (1921). Beads oddly strung. Hartford Herald, 27 April 1921, page 3, 4th column from left.

Hartford Republican (1921) Aurora borealis, The Hartford Republican, 20 May 1921, Front page, bottom of leftmost column

Hartnell, G. (1921). The magnetic storm of May 13–16, 1921, at Cheltenham Observatory, Maryland. *Journal of Geophysical Reaseach*, *26*(1, 2), 25–25. https://doi.org/10.1029/TE026i001p00025-02

Daily Herald (1921). Storm in the Sun. Daily Herald, 18 May 1921, page 8, second column, 5th article.

Hudson, A. E. L. (1921). Auroral display. *Nature*, *107*(2690), 359. https://doi.org/10.1038/107359c0

Hudson, F., Lee, A. M. C., & Mott, F. L. (2000). *American Journalism 1690-1940*, (Vol. 4). London: Routledge. ISBN-13: 978-0415228886

Huurdeman, A. A. (2003). *The worldwide history of telecommunications*. Hoboken, New Jersey: Wiley-Blackwell. ISBN-13: 978-0471205050

IAU (1928) Resolution from commission 4 (Ephemerides) in resolutions from the 3rd General Assembly of the International Astronomical Union, Leiden, July 1928. http://iau.org/static/resolutions/IAU1928_French.pdf (Last accessed 27 April 2019).

Idaho Recorder (1921) This remarkable spring in the Salmon Country, The Idaho Recorder, 27 May 1921, Page 4, leftmost column

Independent-Record (1921). News held up by Aurora Borealis. The Independent-Record (Helena, Montana) · Mon, May 16, 1921 · Page 2

International Telecommunications Union (2007) Ground-wave propagation curves for frequencies between 10 kHz and 30 MHz. International Telecommunications Union recommendation ITU-R P.368-9.

Irumata, T. (1921). The magnetic storm of May 13–17, 1921, at the Meteorological Observatory of Tsingtau, China. *Journal of Geophysical Research*, *26*(3), 112–112. https://doi.org/10.1029/TE026i003p00112-01

Jackson, W. E. W. (1921). Notes from the Meteorological Service: Magnetic disturbances, May 1921. *Journal of the Royal Astronomical Society of Canada*, *15*, 292. ADS Bibliographic Code: 1921JRASC..15..291

Kappenman, J. G. (2006). Great geomagnetic storms and extreme impulsive geomagnetic field disturbance events—An analysis of observational evidence including the great storm of May 1921. *Advances in Space Research*, *38*(2), 188–199. https://doi.org/10.1016/j.asr.2005.08.055

Karsberg, A., Swedenborg, G., & Wyke, K. (1959). *The influences of earth magnetic currents on telecommunication lines*. Tele (English ed.), (pp. 1–21). Stockholm: Televerket.

Krausmann, E., Andersson, E., Gibbs, M., & Murtagh, W. (2016). Space Weather & Critical Infrastructures: Findings and Outlook. EUR 28237 EN. https://doi.org/10.2788/152877

Krausmann, E., Andersson, E., Russel, T., & Murtagh, W. (2015). Space weather and rail: Findings and outlook. EU Joint Research Centre report 98155. doi: https://doi.org/10.2788/211456

Kunitomi, S. I. (1921). The magnetic storm of May 13-17, 1921 as observed at the Kakioka Magnetic Observatory. *Journal of the Meteorological Society of Japan. Ser. I*, *40*(7), en3–en6. https://doi.org/10.2151/jmsj1882.40.7_en3

Lemos, A. (1921). The magnetic storms of March 22–25, 1920, and May 13–17, 1921, at Vassouras Magnetic Observatory, Brazil. *Journal of Geophysical Research*, *26*(3), 96–98. https://doi.org/10.1029/TE026i003p00096

Liu, Y. D., Luhmann, J. G., Kajdič, P., Kilpua, E. K., Lugaz, N., Nitta, N. V., et al. (2014). Observations of an extreme storm in interplanetary space caused by successive coronal mass ejections. *Nature Communications*, *5*(1), 3481. https://doi.org/10.1038/ncomms4481

Lugaz, N., Temmer, M., Wang, Y., & Farrugia, C. J. (2017). The interaction of successive coronal mass ejections: A review. *Solar Physics*, *292*(4).

Lundstedt, H., Persson, T., & Andersson, V. (2015). The extreme solar storm of May 1921: observations and a complex topological model. *Annals of Geophysics*, *33*(1), 109–116. https://doi.org/10.5194/angeo-33-109-2015

Lyman, H. (1921). Remarkable aurora of May 14–15, 1921. *Monthly Weather Review*, *49*(7), 406–409. https://doi.org/10.1175/1520-0493(1921)49%3C406:RAOM%3E2.0.CO;2

Lyot, B. (1921) Aurore boréale dans la nuit du 14 au 15 mai 1921 et phénomènes magnétiques simultanés. *Comptes rendus hebdomadaires des séances de l'Académie des sciences*, *172*, 1230–1231.

Manning Times (1921) No title, The Manning Times, 18 May 1921, Page 8, second column from left, 6th paragraph

Matin (1921). C'est un orage qui a troublé l'autre nuit nos transmissions télégraphiques. Le Matin, 17 May 1921, front page, top of 5th column.

Mitchell, A. C. (1921). The Magnetic Storm of May 13–17. *Nature*, *107*(2691), 392–393. https://doi.org/10.1038/107392c0

National Science and Technology Council (2018) Space Weather Phase 1 Benchmarks, https://www.whitehouse.gov/wp-content/uploads/2018/06/Space-Weather-Phase-1-Benchmarks-Report.pdf Last accessed 1 February 2019.

Nevanlinna, H. (1997). Gauss' H-Variometer at the Helsinki Magnetic Observatory 1844-1912. *Journal of Geomagnetism and Geoelectricity*, *49*(10), 1209–1215. https://doi.org/10.5636/jgg.49.1209

Newton, H. W. (1948). "Sudden commencements" in the Greenwich magnetic records (1879–1944) and related sunspot data. Geophysical Supplements to the. *Monthly Notices of the Royal Astronomical Society*, *5*(6), 159–185. https://doi.org/10.1111/j.1365-246X.1948.tb02933.x

Ngwira, C. M., Pulkkinen, A., Leila Mays, M., Kuznetsova, M. M., Galvin, A. B., Simunac, K., et al. (2013). Simulation of the 23 July 2012 extreme space weather event: What if this extremely rare CME was Earth directed? *Space Weather*, *11*, 671–679. https://doi.org/10.1002/2013SW000990

NYT (1921a). Sunspot Aurora Paralyses Wires, New York Times, 15 May 1921, front page.

NYT (1921b). Sunspot Credited with Rail Tie-Up, New York Times, 16 May 1921, page 2.

NYT (1921c). Cables Damaged by Sunspot Aurora, New York Times, 17 May 1921, front page.

NYT (1921d). Magnetic Storms Don't Affect Radio, New York Times, 26 May 1921, page 18.

NYT (1921e). Northern Lights are Busy, New York Times, 14 May 1921, page 10.

NYT (1921f). Electric disturbances affect French wires, New York Times, 18 May 1921, page 12.

O. de l'Ebre (2019) International service on rapid magnetic variations, SSC Table for 1921, http://www.obsebre.es/php/geomagnetisme/vrapides/ssc_1921_d.html

OECD (2018). *National risk assessments: A cross country perspective*. Paris: OECD Publishing. https://doi.org/10.1787/9789264287532-en

Omaha Daily Bee (1921). Wires put out of order by aurora, The Omaha Daily Bee, 16 May 1921, Front page, 3rd column from left.

Ottawa Journal (1921). Pesky Aurora Borealis burns out telephones, Ottawa Journal, 17 May 1921, page 15, fifth column from left.

Oughton, E. J., Hapgood, M., Richardson, G. S., Beggan, C. D., Thomson, A. W., Gibbs, M., et al. (2018). A risk assessment framework for the socioeconomic impacts of electricity Transmission infrastructure failure due to space weather: An application to the United Kingdom. *Risk Analysis*, *39*(5), 1022–1043. https://doi.org/10.1111/risa.13229

Parkinson, W. C. (1921). The magnetic storm of 13–17 May 1921, at Watheroo Observatory, Australia. *Journal of Geophysical Research*, *26*(1, 2), 26–28. https://doi.org/10.1029/TE026i001p00026-02

Prescott Journal-Miner (1921) Sunspots cause aurora, says Updegraff. His observations, Prescott Journal-Miner, 18 May 1921, Front page, bottom of page in 3rd and 4th columns from left

Ptitsyna, N. G., Sokolov, S. N., Soldatov, V. A., & Tyasto, M. I. (2018). Historical database of geomagnetic and auroral activity for the study of solar-terrestrial relationships. *Izvestiya, Atmospheric and Oceanic Physics*, *54*(7), 730–737. https://doi.org/10.1134/S0001433818070095

Pulkkinen, A., Bernabeu, E., Thomson, A., Viljanen, A., Pirjola, R., Boteler, D., et al. (2017). Geomagnetically induced currents: Science, engineering, and applications readiness. *Space Weather*, *15*, 828–856. https://doi.org/10.1002/2016SW001501

Rock Island Argus (1921a) Freak of sky cuts off city wire service, Rock Island Argus, 16 May 1921, Page7, leftmost column

Rodes, F. L. (1921). The magnetic storm of May 13–16, 1921, at Observatorio del Ebro, Tortosa, Spain. *Journal of Geophysical Research*, *26*(1, 2), 26–26. https://doi.org/10.1029/TE026i001p00026-01

Royal Greenwich Observatory. (1955). Sunspot and geomagnetic-storm data: derived from Greenwich observations, 1874-1954. HM Stationery Off..

Russell, H. N., Slipher, V. M., & Lampland, C. O. (1921). Observations of the aurora at the Lowell Observatory May 14, 1921. *Science*, *54*(1392), 183–187. https://doi.org/10.1126/science.54.1392.183

Saiz, E., Guerrero, A., Cid, C., Palacios, J., & Cerrato, Y. (2016). Searching for Carrington-like events and their signatures and triggers. *Journal of Space Weather and Space Climate*, *6*, A6. https://doi.org/10.1051/swsc/2016001

San Bernardino Daily Sun (1921) Arctic Lights are Brilliant out in the Desert, San Bernardino Daily Sun, 16 May 1921, Front page, 4th column from left

Sanders, R. (1961). Effect of terrestrial electromagnetic storms on wireline communications. *IRE Transactions on Communications Systems*, *9*(4), 367–377. https://doi.org/10.1109/TCOM.1961.1097724

Sheffield Independent (1921). Northern Lights: Record display affects Sweden's telephones Sheffield Independent, Monday 16 May 1921, front page, column 6.

Silverman, S. M., & Cliver, E. W. (2001). Low-latitude auroras: The magnetic storm of 14–15 May 1921. *Journal of Atmospheric and Solar-Terrestrial Physics*, *63*(5), 523–535. https://doi.org/10.1016/S1364-6826(00)00174-7

Siscoe, G., Crooker, N. U., & Clauer, C. R. (2006). Dst of the Carrington storm of 1859. *Advances in Space Research*, *38*(2), 173–179. https://doi.org/10.1016/j.asr.2005.02.102

Skey, H. F. (1921). The recent magnetic storm, 14th to 17th May, 1921. *New Zealand Journal of Science and Technology*, *4*, 197–201.

Springfield Republican (1921) High Voltage From the Skies. Springfield Republican, 23 May 1921, page 6, column 3.

Stenquist, D. (1925), Etude des courants telluriques, Mémoires publiés par la Direction Générale des Télégraphes de Suède, Stockholm (printed by R.W. Statlanders boktryckeri)

Stewart, B. (1861). On the great magnetic disturbance which extended from August 28 to September 7, 1859, as recorded by photography at the Kew Observatory. *Philosophical Transactions of the Royal Society of London*, *151*, 423–430. https://doi.org/10.1098/rstl.1861.0023

Sunderland Daily Echo (1921) Sunspot effects, sunderland daily echo, 18 May 1921, page 6. Bottom of 3rd column.

Tamm, N. (1922). Die großen Sonnenflecken Mitte Mai und Anfang Juni 1921. *Astronomische Nachrichten*, *215*(8), 209–212. https://doi.org/10.1002/asna.19212150804

Telegraph and Telephone Age (1921a) Notes on observations of aurora or Earth current effect on telegraph wires at Capreol, May 14th, Telegraph and Telephone Age 39, 273 (16 June 1921)

Telegraph and Telephone Age (1921b) Radio aurora proof, Telegraph and Telephone Age 39, 264 (1 June 1921)

Telegraph and Telephone Age (1921c) The Recent Electrical Disturbances, Telegraph and Telephone Age 39, 244 (1 June 1921)

Thébault, E., Finlay, C. C., Beggan, C. D., Alken, P., Aubert, J., Barrois, O., et al. (2015). International geomagnetic reference field: the 12th generation. Earth. *Planets and Space*, *67*(1), 79. https://doi.org/10.1186/s40623-015-0228-9

Wilkens, A., & Emde, K. (1921). Über das Nordlicht vom 13. und 14. Mai 1921. *Astronomische Nachrichten*, *213*(23), 383–384. https://doi.org/10.1002/asna.19212132306

Wilson, M. (1921). Summary of Mount Wilson Magnetic Observations of Sun-spots for May and June, 1921. *Publications of the Astronomical Society of the Pacific*, *22*, 209–211. https://doi.org/10.1086/123087

References From the Supporting Information

Araki, T., Funato, K., Iguchi, T., & Kamei, T. (1993). Direct detection of solar wind dynamic pressure effect on ground geomagnetic field. *Geophysical Research Letters*, *20*(9), 775–778. https://doi.org/10.1029/93GL00852

Araki, T., & Shinbori, A. (2016). Relationship between solar wind dynamic pressure and amplitude of geomagnetic sudden commencement (SC). *Earth, Planets and Space*, *68*(1), 90.

Arizona Republican (1921b). Arrangements for Dempsey-Carpentier Go are finished. The Arizona Republican, 29 April 1921, front page, 6th column from left

Brewster Standard (1921b). Daylight saving recommended, Brewster Standard, 22 April 1921, front page, rightmost column, second article.

Cliver, E. W., Feynman, J., & Garrett, H. B. (1990). An estimate of the maximum speed of the solar wind, 1938–1989. *Journal of Geophysical Research*, *95*(A10), 17,103–17,112. https://doi.org/10.1029/JA095iA10p17103

Rock Island Argus (1921b). Daylight schedule, rock island argus, 26 March 1921, front page, 3rd column from left, penultimate item.

Siscoe, G. L., Formisano, V., & Lazarus, A. J. (1968). Relation between geomagnetic sudden impulses and solar wind pressure changes—An experimental investigation. *Journal of Geophysical Research*, *73*(15), 4869–4874. https://doi.org/10.1029/JA073i015p04869